Master thesis Wilhelm Coupled Cluster

by

Fredrik Wilhelm Holmen

Thesis

for the degree of

Master of Science

Faculty of Mathematics and Natural Sciences
University of Oslo

Autumn 2015

Abstract

This is an abstract text.

To someone

Acknowledgements

I acknowledge my acknowledgements.

Contents

1 Introduction **1**

2 Quantum Mechanics **3**
- 2.1 Postulates . . . 3
- 2.2 The Born-Oppenheimer Approximation . . . 4
- 2.3 Pauli's Exclusion Principle . . . 4
- 2.4 The Variational Principle . . . 5
- 2.5 Slater Determinant . . . 5
- 2.6 Matrix Elements . . . 5

3 Second Quantization **7**
- 3.1 Annihilation and Creation operators . . . 7
- 3.2 Strings of Operators . . . 8
- 3.3 Anticommutator Relations . . . 9
- 3.4 Inner products . . . 10
- 3.5 Representation of Operators . . . 11
  - 3.5.1 One-Body Operator . . . 11
  - 3.5.2 Two-body Operator . . . 13
  - 3.5.3 The Hamiltonian . . . 14
- 3.6 Normal Ordering and Wick's Theorem . . . 14
  - 3.6.1 Normal Ordering . . . 14
  - 3.6.2 Contractions . . . 15
  - 3.6.3 Time-independent Wick's theorem . . . 15
- 3.7 Particle-Hole Formulation . . . 16
- 3.8 Normal ordering of Operators . . . 17
  - 3.8.1 One-Body Operator . . . 17
  - 3.8.2 Two-Body operators . . . 18
- 3.9 Partitioning the Hamiltonian Operator . . . 19
- 3.10 Normal Ordering of Hamiltonian . . . 21
- 3.11 Correlation Energy . . . 22

4 Diagramatic Representation **25**
4.1 The Slater Determinant . . . 25
4.2 Operators . . . 26
4.3 Contractions and Inner products . . . 30
4.4 Interpreting Diagrams . . . 32
4.5 Linked Diagram theorem . . . 32

5 Many-Body Methods **33**
5.1 Full Configuration Interaction Theory . . . 34
5.1.1 The Hamiltonian Matrix . . . 35
5.1.2 Computational cost . . . 36
5.2 Many-body Perturbation Theory . . . 36
5.2.1 General derivation of Many Body Particle Theory equations 37
5.2.2 Equations for Reileigh-Schrodinger Perturbation Theory . 38
5.3 Hartree-Fock calculations . . . 40

6 Coupled-Cluster Theory **43**
6.1 Size Extensivity . . . 44
6.2 The CCD Equations . . . 44
6.3 Intermediates . . . 46

7 The Pairing Model **49**
7.1 The Hamiltonian . . . 50
7.2 Configuration Interaction theory . . . 51
7.3 Hartree-Fock calculations . . . 53
7.4 Many-Body Perturbation Theory . . . 54
7.4.1 Interpreting diagrams . . . 55
7.4.2 Label all lines . . . 56
7.4.3 Identify the operators . . . 56
7.4.4 Identify the denominator . . . 56
7.4.5 Including phase factor . . . 57
7.4.6 Identify equivalent lines . . . 57
7.4.7 Second Order Perturbation Theory . . . 57
7.4.8 Third Order Perturbation Theory . . . 57
7.4.9 Fourth Order Perturbation Theory . . . 58
7.5 Spin Summations . . . 63

8 Infinite Matter **65**
8.1 The Infinate Electron Gas . . . 65
8.1.1 The Hamiltonian . . . 65
8.1.2 The Reference Energy . . . 67
8.1.3 The Fock Matrix Elements . . . 67
8.1.4 Anti-Symmetric Matrix Elements . . . 68

8.1.5 The Plane Wave Basis . . . 68
8.2 Infinite Nuclear Matter . . . 71
8.3 Nuclear Interaction . . . 71
8.3.1 The Minnesota Potential . . . 71

9 Implementation of CCD **73**
9.1 Implementing the CCD equations . . . 73
9.2 Matrix Representation of Contractions . . . 74
9.2.1 Aligning elements . . . 75
9.3 Block Implementation . . . 77
9.3.1 Two-state configurations . . . 78
9.3.2 Unaligned channels . . . 79
9.3.3 Permutations . . . 82
9.4 Setting Up Basis . . . 82
9.5 Parallellization . . . 82

10 Results **85**
10.1 The Pairing Model . . . 85
10.1.1 Comparison of CCD solvers . . . 86
10.1.2 Comparison of various solvers . . . 87

11 Conclusion and future prospects **91**

Chapter 1

Introduction

In this thesis, I have calculated the ground state energy for the pairing model, homogenous electron gas and infinite nuclear matter. My main focus has been to implement the coupled cluster method with double excitations

Chapter 2

Quantum Mechanics

2.1 Postulates

Quantum mechanics is built upon by a few principles [2, 5, 6, 9], often called the postulates of quantum mechanics.

1. **The Wave Function**
   All information on a quantum system is given by the wave function $|\Psi(x,t)\rangle$. The wave function represent the probability of measuring a particle within a small volume dx and for a given time, t. As the probability cannot exceed 1, the wave function must be normalized, namely

   $$\int_{-\infty}^{\infty} \Psi^*(x,t)\Psi(x,t)\mathrm{dx} = 1 \tag{2.1}$$

   Physical distinguishable states are orthogonal to each other. Using normalized states, they are orthonormal to each other, meaning that for two unambigously distuingishable states, we have

   $$\langle\lambda|\psi\rangle = \delta_{\lambda\psi} \tag{2.2}$$

2. **Observables**
   All observables are represented by linear operators, written with a "hat", $\hat{O}$. These linear operators are bound to be hermitian. An observable could also be called measurable quality. The outcome of a quantum mechanical experiment is an observable.

3. **Measurments**
   The possible outcomes of an experminent are the eigenvalues of an operator that represent the observable. Represented as a number λ. If a state is in the eigenstate $|\lambda\rangle$, the only possible measurment of an experiment is the

eigenvalue, λ. We write this as

$$\hat{O}\,|\lambda\rangle = \lambda\,|\lambda\rangle \tag{2.3}$$

4. **Probabilities**
   Given a state $|\alpha\rangle$. The probability of observing λ when measuring the observable $\hat{O}$ is given by

   $$P(\lambda) = \langle\alpha|\lambda\rangle\,\langle\lambda|\alpha\rangle = |\,\langle\alpha|\lambda\rangle\,|^2 \tag{2.4}$$

   Which measures the overlap of the two states $|\alpha\rangle$ and $|\lambda\rangle$. If they are physically distinguishable, the probability is zero. If the probability is non-zero, we have "mixed states".

5. **Time development and the Schrodinger equation**
   Time developement for states are given by acting on the state with a unitary operator

   $$|\Psi(t)\rangle = \hat{U}(t)\,|\Psi(0)\rangle \tag{2.5}$$

   This leads us to the time-independent Schrodinger equation

   $$\hat{H}\,|\Psi(x,t)\rangle = i\hbar\frac{\partial}{\partial t}\,|\Psi(x,t)\rangle \tag{2.6}$$

   Where we have defined the Hamiltonian operator $\hat{H}$. The Hamiltonian will be used throughout the thesis, as its eigenvalues are the measurable energy. We will primerily be focused on solving the *time independent* Schrodinger equation

   $$\hat{H}\,|\Psi(x)\rangle = E\,|\Psi(x)\rangle \tag{2.7}$$

2.2 The Born-Oppenheimer Approximation

The Born-Oppenheimer approximation lies at the heart of many-body quantum mechanics.

2.3 Pauli's Exclusion Principle

Pauli exclusion principle, also called the antisymmetry principle [4]

2.4 The Variational Principle

2.5 Slater Determinant

A system composed of a nuclei and electrons moving in accordance to the forces of electromagnetic attraction can be described by assigning each electron a wave function

$$\phi_i(\mathbf{x}_i) \tag{2.8}$$

Where $\mathbf{x}_i$ is the position vector for the electron i. Describing a system of many electrons can be done writing a Slater Determinant

$$|\Phi_0\rangle = \frac{1}{\sqrt{N!}} \begin{vmatrix} \phi_1(\mathbf{x}_1) & \phi_2(\mathbf{x}_1) & ... & \phi_N(\mathbf{x}_1) \\ \phi_1(\mathbf{x}_2) & \phi_2(\mathbf{x}_2) & ... & \phi_N(\mathbf{x}_2) \\ ... & & & \\ \phi_1(\mathbf{x}_N) & \phi_2(\mathbf{x}_N) & ... & \phi_N(\mathbf{x}_N) \end{vmatrix} \tag{2.9}$$

This way of writing the many-body wave function will represent linear a combination of products of the one-body wave functions ϕ_i's and all the electronic coordinates $\mathbf{x}_i$ distributed among them in all possible ways. Exchanging two lines will change the sign such that the Slater Determinant will respect the antisymmetry requirement.

We can choose the one-body wave functions that is most rewarding the specified system. When calculating on electrons moving with respect to a nuclei, one can choose the wave functions to be the 1s, 2s, 2p, .. orbitals. This representation will not, however, take into account the Colombic repulsion between two electrons and will only be an approximation to the true wavefunction, $|\Psi\rangle$.

2.6 Matrix Elements

Chapter 3

Second Quantization

Second quantization is a new method of representing states and operators.

3.1 Annihilation and Creation operators

We introduce a new way of writing states using the mathematical technique known as second quantization. The main goal is to treat states without paying attention to individual particle coordinates. We represent the empty space with the symbol for vacuum

$$|0\rangle \tag{3.1}$$

To represent a state, we use a creation operator to add the state to the vacuum.

$$\hat{a}_i^\dagger |0\rangle = |\phi_i\rangle \tag{3.2}$$

And the annihilation operator will remove the particle again.

$$\hat{a}_i |\phi_i\rangle = |0\rangle \tag{3.3}$$

Trying to add a new particle to an already filled state and removing an unoccupied state results in zero.

$$\hat{a}_i^\dagger |\phi_i\rangle = 0 \qquad \hat{a}_i |0\rangle = 0 \tag{3.4}$$

Bra states are needed, and by looking at the adjoint of a ket state, we get

$$(|\phi_i\rangle)^\dagger = \langle\phi_i| \tag{3.5}$$

Which results in

$$\left(\hat{a}_i^\dagger \left|0\right\rangle\right)^\dagger = \left\langle 0\right| \hat{a}_i = \left\langle \phi_i \right| \tag{3.6}$$

We see that the creation and annihilator operatorare each other's adjoint operator. We can define the counting operator, $\hat{N}$, which will count how many states are occupied in a Slater determinant

$$\hat{N} = \sum_p \hat{a}_p^\dagger \hat{a}_p = \sum_p \hat{n}_p \tag{3.7}$$

3.2 Strings of Operators

We can now construct the Slater determinant by working on vacuum with a string of creation operators

$$\hat{a}_1^\dagger \hat{a}_2^\dagger ... \hat{a}_N^\dagger \left|0\right\rangle = \left|\phi_1 \phi_2 ... \phi_N\right\rangle \tag{3.8}$$

Permutations of the operators introduces a sign-change, which is equivalent to interchanging rows in the determinant. We need second quantization to respect the anisymmetrization condition, so a permutation of two states should introduce a change of sign

$$\hat{a}_1^\dagger \hat{a}_2^\dagger \left|0\right\rangle = \left|\phi_1 \phi_2\right\rangle = -\left|\phi_2 \phi_1\right\rangle = -\hat{a}_2^\dagger \hat{a}_1^\dagger \left|0\right\rangle \tag{3.9}$$

We introduce the permutation operator, $\hat{P}$, which permutes two states in the Slater determinant

$$\hat{P}\left|\Phi\right\rangle = (-1)^{\sigma(P)} \left|\Phi\right\rangle \tag{3.10}$$

Where $\sigma(P)$ counts how many times the states are interchanged. Demonstrated with creation operators

$$\hat{a}_1^\dagger \hat{a}_2^\dagger ... \hat{a}_i^\dagger \hat{a}_j^\dagger ... \hat{a}_n^\dagger = -\hat{a}_1^\dagger \hat{a}_2^\dagger ... \hat{a}_j^\dagger \hat{a}_i^\dagger ... \hat{a}_n^\dagger \tag{3.11}$$

3.3 Anticommutator Relations

When working on strings of operators, it is very convenient to introduce anti-commutator relations. We define the relation as

$$\{\hat{A}, \hat{B}\} = \hat{A}\hat{B} + \hat{B}\hat{A} \tag{3.12}$$

By inserting the annihilation and creation operator, we can compute the relations and look at how they work on the vacuum state

$$\{\hat{a}_i^\dagger \hat{a}_j\} |0\rangle = \hat{a}_i^\dagger \hat{a}_j |0\rangle + \hat{a}_j \hat{a}_i^\dagger |0\rangle = 0 + \delta_{ij} |0\rangle \tag{3.13}$$

Where we have introduced the kroenecker-delta function

$$\delta_{ij} = \begin{cases} 1, & \text{if } i = j \\ 0, & \text{ij } i \neq j \end{cases} \tag{3.14}$$

The second case

$$\{\hat{a}_i \hat{a}_j^\dagger\} |0\rangle = \hat{a}_i \hat{a}_j^\dagger + \hat{a}_j^\dagger \hat{a}_i |0\rangle = \delta_{ij} |0\rangle + 0 \tag{3.15}$$

And the two last cases

$$\{\hat{a}_i \hat{a}_j\} |0\rangle = \hat{a}_i \hat{a}_j |0\rangle + \hat{a}_j \hat{a}_i |0\rangle = \hat{a}_i \hat{a}_j |0\rangle - \hat{a}_i \hat{a}_j |0\rangle = 0 \tag{3.16}$$

$$\{\hat{a}_i^\dagger \hat{a}_j^\dagger\} |0\rangle = \hat{a}_i^\dagger \hat{a}_j^\dagger |0\rangle + \hat{a}_j^\dagger \hat{a}_i^\dagger |0\rangle = \hat{a}_i^\dagger \hat{a}_j^\dagger |0\rangle - \hat{a}_i^\dagger \hat{a}_j^\dagger |0\rangle = 0 \tag{3.17}$$

Ending up with our relations

$$\{\hat{a}_i \hat{a}_j\} = 0 \tag{3.18}$$

$$\{\hat{a}_i^\dagger \hat{a}_j^\dagger\} = 0 \tag{3.19}$$

$$\{\hat{a}_i^\dagger \hat{a}_j\} = \{\hat{a}_i \hat{a}_j^\dagger\} = \delta_{ij} \tag{3.20}$$

The last result is very useful for rewriting strings of operators, since it allows us to rewrite a set of two operators as

$$\hat{a}_i^\dagger \hat{a}_j = \{\hat{a}_i^\dagger \hat{a}_j\} - \hat{a}_j \hat{a}_i^\dagger = \delta_{ij} - \hat{a}_j \hat{a}_i^\dagger \tag{3.21}$$

Which will be at the center of Wick's theorem.

3.4 Inner products

We assume all states are orthonormal, taking the inner product of two states should give

$$\langle i|j\rangle = \delta_{ij} \tag{3.22}$$

And for consistency, the vacuum state must also be normalized

$$\langle 0||0\rangle = 1 \tag{3.23}$$

this can be demonstrated by looking at the definition of the inner product of two equal states and using the anticommutator relations

$$1 = \langle i|i\rangle = \left\langle 0|\hat{a}_i\hat{a}_i^\dagger|0\right\rangle \tag{3.24}$$

$$= \left\langle 0|(\delta_{ij} - \hat{a}_i^\dagger\hat{a}_i)|0\right\rangle \tag{3.25}$$

$$= \langle 0|0\rangle - 0 = \langle 0|0\rangle \tag{3.26}$$

It turns out we can use this exact scheme for longer chains of operators as well. Looking at the inner product of two general Slater Determinants

$$|A\rangle = |a_1a_2...a_N\rangle = \hat{a}_1^\dagger\hat{a}_2^\dagger...\hat{a}_N^\dagger\,|0\rangle \tag{3.27}$$

$$|B\rangle = |b_1b_2...b_N\rangle = \hat{b}_1^\dagger\hat{b}_2^\dagger...\hat{b}_N^\dagger\,|0\rangle \tag{3.28}$$

Writing the inner product

$$\langle A|B\rangle = \left\langle 0|\hat{a}_N...\hat{a}_2\hat{a}_1\hat{b}_1^\dagger\hat{b}_2^\dagger...\hat{b}_N^\dagger|0\right\rangle \tag{3.29}$$

By moving the annihilation operators all the way to the right, we know that the inner product becomes zero because $\hat{a}_p\,|0\rangle = 0$. We utilize the anticommutator relations for interchanging creation and annihilation operators shown in (3.21). By first moving a_1 to the right, we get two possible outcomes

1. One b_p is equal to a_1 and we get

$$\hat{a}_1\hat{b}_p^\dagger = \delta_{a_1,b_p} - \hat{b}_p^\dagger\hat{a}_1 = 1 - \hat{b}_p^\dagger\hat{a}_1 \tag{3.30}$$

This will now give us a new and shorter inner product

$$\langle A|B\rangle = \langle 0|\,\hat{a}_N...\hat{a}_2\hat{b}_1^\dagger...\hat{b}_{p-1}^\dagger\hat{b}_{p+1}^\dagger...\hat{b}_N^\dagger\,|0\rangle\,(-1)^{p-1} - \langle 0|\,\hat{a}_N...\hat{a}_2\hat{b}_1^\dagger\hat{b}_2^\dagger...\hat{b}_N^\dagger\hat{a}_1\,|0\rangle \tag{3.31}$$

Where the last term will vanish because of $\hat{a}_1\,|0\rangle = 0$. Notice the sign factor

coming from $(-1)^{p-1}$. This is due to interchanging creation operators when moving $\hat{b}_p^\dagger$ from position p and $(p-1)$ steps to the left before using (3.30).

2. No b_p is equal to a_1 and all $\delta_{a_1,b_p} = 0$. Applying the same logic as for outcome 1, we get

$$\langle A|B\rangle = 0 \tag{3.32}$$

We do the same for all states and see that this inner product can only be non-zero if all states $a_1..a_N$ has a matching state in $b_1..b_N$ and vice versa. If the ordering of states is different, a permutation factor $-1^{\sigma(P)}$ is included.

3.5 Representation of Operators

Consider a symmetric one-body operator represented by

$$\hat{F} = \sum_{\mu=1}^{N} \hat{f}_\mu \tag{3.33}$$

The number μ tells us on which particle $\hat{F}$ works on. In this case, we are looking at a symmetric operator because it works identically on all particles. Looking at a matrix element of $\hat{F}$ put petween two Slater determinants.

$$\langle a_1 a_2 ... a_N| \hat{F} |b_1 b_2 ... b_N\rangle \tag{3.34}$$

$$\sum_\mu \langle a_1 a_2 ... a_N| \hat{f}_\mu |b_1 b_2 ... b_N\rangle \tag{3.35}$$

3.5.1 One-Body Operator

In second quantization, a one-body operator is given as

$$\hat{F} = \sum_{pq} \langle p| \hat{f} |q\rangle \hat{a}_p^\dagger \hat{a}_q \tag{3.36}$$

Where the matrix element $\langle p| \hat{f} |q\rangle$ is determined on the nature of the operator $\hat{F}$. It is common to denote this matrix element as

$$\hat{F} = \sum_{pq} \langle p| \hat{f} |q\rangle \hat{a}_p^\dagger \hat{a}_q = \sum_{pq} f_{pq} \hat{a}_p^\dagger \hat{a}_q \tag{3.37}$$

Doing calculations in many-body quantum mechanics, we are primerely interested in expectation values. It is therefore crucial that we develop a solid scheme for calculating these values. This can be done by for example looking at the following inner product

$$\langle P|\,\hat{F}\,|R\rangle \tag{3.38}$$

Inserting the definition of $\hat{F}$

$$\langle 0|\,\hat{a}_M...\hat{a}_s\hat{a}_r\left(\sum_{kl} f_{kl}\hat{a}_k^\dagger\hat{a}_l\right)\hat{a}_p^\dagger\hat{a}_q^\dagger...\hat{a}_N^\dagger\,|0\rangle \tag{3.39}$$

Which can be rewritten as

$$\sum_{pq} f_{pq}\,\langle 0|\,\hat{a}_M...\hat{a}_s\hat{a}_r(\hat{a}_k^\dagger\hat{a}_l)\hat{a}_p^\dagger\hat{a}_q^\dagger...\hat{a}_N^\dagger\,|0\rangle \tag{3.40}$$

We apply the same logic as in the previous section, which provides us with three different outcomes for this expectation value

1. The states $p, q, ..., N$ are all identical to the states $r, s, ..., M$. This results in

$$\langle P|\,\hat{F}\,|R\rangle = \sum_k^N f_{kk}(-1)^{\sigma(P)} \tag{3.41}$$

   Where we have included a perturbation factor in case the ordering of states is different in the two states.

2. If all states except one from each Slater determinant are equal, we get a *noncoincidence* [3]

$$(p = r),\ (s = q),\ ...,\ (n \neq m),\ ...,\ (N = N) \tag{3.42}$$

   we can rewrite the expectation value as

$$\sum_{pq} f_{pq}\,\langle 0|\,\hat{a}_M...\hat{a}_s\hat{a}_r(\hat{a}_k^\dagger\hat{a}_l)\hat{a}_p^\dagger\hat{a}_q^\dagger...\hat{a}_N^\dagger\,|0\rangle = (-1)^{\sigma(P)}f_{mn} \tag{3.43}$$

   Because the operators $\hat{a}_k^\dagger$ and $\hat{a}_l$ must be paired with the non-identical states m and n for us to be left with a orthogonal inner product.

3. If there are more than one noncoincidence, no contributions can survive,

and the expectation value is

$$\langle P|\,\hat{F}\,|R\rangle = 0 \tag{3.44}$$

3.5.2 Two-body Operator

I have in this thesis only looked at Hamiltonians consisting of a maximum of two-body interactions. Because of this, I will need a formalism for a two-body operator as well. It is defined almost identically as the one-body operator. We write the general two-body operator as

$$\hat{G} = \frac{1}{2}\sum_{ijkl}\langle i(1)j(2)|\,g_{12}\,|k(1)l(2)\rangle\,\hat{a}_i^\dagger\hat{a}_j^\dagger\hat{a}_l\hat{a}_k \tag{3.45}$$

Where the numbers (1) and (2) show which particle occupy the what state. We are, as for the one-body operator, interested in how we can calculate expectation values for this operator. We take the inner product with the SD's $|P\rangle$ and $|R\rangle$.

$$\frac{1}{2}\sum_{ijkl}\langle i(1)j(2)|\,g_{12}\,|k(1)l(2)\rangle\,\langle 0|\,\hat{a}_M...\hat{a}_s\hat{a}_r(\hat{a}_i^\dagger\hat{a}_j^\dagger\hat{a}_l\hat{a}_k)\hat{a}_p^\dagger\hat{a}_q^\dagger...\hat{a}_N^\dagger\,|0\rangle \tag{3.46}$$

There are three possible outcomes here as well

1. If there are none noncoincidences, and all states in SD $|P\rangle$ is equal to all states in SD $|R\rangle$, we get

$$\langle P|\,\hat{G}\,|R\rangle = \frac{1}{2}\sum_{p\in P}\sum_{q\in P}(\langle pq|\,\hat{g}\,|pq\rangle - \langle pq|\,\hat{g}\,|qp\rangle) = \frac{1}{2}\sum_{p\in P}\sum_{q\in P}\langle pq||pq\rangle \tag{3.47}$$

   Where it is useful to use the antisymmetric matrix element

$$\langle pq||pq\rangle = \langle pq|\,\hat{g}\,|pq\rangle - \langle pq|\,\hat{g}\,|qp\rangle \tag{3.48}$$

2. If we have a single noncoincidence, where all states except one from each SD are perfectly identical, we get [3]

$$\langle P|\,\hat{G}\,|R\rangle = \sum_{q\in P}\langle p'q||pq\rangle \tag{3.49}$$

   where the states p' and p are the unequal states.

3. If we have two noncoincidences, we get

$$\langle P|\,\hat{G}\,|R\rangle = \langle p'q'||pq\rangle \tag{3.50}$$

4. If more than two states from each SD are unequal, the expectation value will be 0.

3.5.3 The Hamiltonian

We can now write our Hamiltonian using second quantization. The Hamiltonian consist of a one-body and a two-body term

$$\hat{H} = \hat{H}_1 + \hat{H}_2 \tag{3.51}$$

Which can be written out as

$$\hat{H}_1 = \sum_{\mu} \hat{h}_{\mu}, \qquad \hat{H}_2 = \sum_{\mu<\nu} \hat{v}_{\mu\nu} \tag{3.52}$$

Using atomic units, we can write this as

$$\hat{h}_{\mu} = -\frac{1}{2}\nabla_{\mu}^2 - \sum_{A} \frac{Z_A}{r_{\mu A}}, \qquad \hat{v}_{\mu\nu} = \frac{1}{r_{\mu\nu}} \tag{3.53}$$

Using the formalism introduced, we can write this as

$$\hat{H} = \hat{H}_1 + \hat{H}_2 = \sum_{ij} \langle i| \hat{h} |j\rangle \hat{a}_i^{\dagger}\hat{a}_j + \frac{1}{4}\sum_{ijkl} \langle ij||kl\rangle \hat{a}_i^{\dagger}\hat{a}_j^{\dagger}\hat{a}_l\hat{a}_k \tag{3.54}$$

Where we have used the anti-symmetric form of the two-body operator

$$\langle ij||kl\rangle = \langle i(1)j(2)| \hat{v}_{12} |k(1)l(2)\rangle - \langle i(1)j(2)| \hat{v}_{12} |l(1)k(2)\rangle \tag{3.55}$$

3.6 Normal Ordering and Wick's Theorem

As one can see, calculations of inner products can be a tedious affair when utilizing the anitcommutator rules. Luckily, one can develop more powerful tools, namely Wick's theorem. Before introducing Wick's theorem, a definition of normal ordering and contractions are needed

3.6.1 Normal Ordering

As previously shown, when evaluating a string of operators, the general scheme is to place all annihilation operators to the right of creation operators. This is because, when working on the true vacuum state, annihilation operators give

zero. The only non-zero results will then arize from kroenecker delta's when permutating creation-annihilation operators according to (3.21).

A string of operators with all annihilation operators to the right will be referred to as a *normal ordered* string of operators. Normal ordering of operators is commonly denoted by a curvy bracket or square bracket

$$n[\hat{A}\hat{B}...\hat{N}] = \{\hat{A}\hat{B}...\hat{N}\} \tag{3.56}$$

Any expectation value, with respect to the true vacuum, of a set of normal ordered operators will always be zero

$$\langle 0|\,\{\hat{A}\hat{B}...\hat{N}\}\,|0\rangle = 0 \tag{3.57}$$

One can note that the Hamiltonian operator is already written in a *normal ordered* form.

3.6.2 Contractions

The second tool needed for Wick's theorem is the definition *contractions* of operators. We define the contraction of general creation and annihilation operators as

$$\hat{A}\hat{B} \equiv \hat{A}\hat{B} - \{\hat{A}\hat{B}\} \tag{3.58}$$

Before taking the expactation value of the two operators with respect to the true vacuum. Giving the results

$$\hat{a}_a^\dagger \hat{a}_b^\dagger = \hat{a}_a \hat{a}_b = \hat{a}_a^\dagger \hat{a}_b = 0 \tag{3.59}$$

The only non-zero results will be for

$$\hat{a}_a \hat{a}_b^\dagger = \delta_{ab} \tag{3.60}$$

3.6.3 Time-independent Wick's theorem

Wick's theorem states: *A product of a string of creation and annihilation operators is equal to their normal product plus the sum of all possible normal ordered contractions* [3]. Symbolically, this is shown by

$$\hat{A}\hat{B}\hat{C}\hat{D}... = \{\hat{A}\hat{B}\hat{C}\hat{D}...\} + \sum \{\underbrace{A\hat{B}\hat{C}\hat{D}....}\} \tag{3.61}$$

The usefulness of this relation is when calculating expectation values. Because of (3.57), the only result that will give a non-zero result, is when all operators are fully contracted. As an example to display the usefulness of Wick's theorem

$$\langle 0|\, \hat{a}_a \hat{a}_b^\dagger \hat{a}_c \hat{a}_d^\dagger \hat{a}_e \hat{a}_f^\dagger \,|0\rangle = \langle 0|\, \{\hat{a}_{\underbrace{a}} \hat{a}_{\underbrace{b}}^\dagger \hat{a}_{\underbrace{c}} \hat{a}_{\underbrace{d}}^\dagger \hat{a}_{\underbrace{e}} \hat{a}_{\underbrace{f}}^\dagger\} \,|0\rangle = \delta_{ab}\delta_{cd}\delta_{ef} \tag{3.62}$$

Where the contractions displayed are the only set of non-zero contractions possible.

3.7 Particle-Hole Formulation

For larger Slater determinants, it is tedious to write all states in terms of the vacuum state $|0\rangle$. We define a reference state that will be used instead of the pure vacuum. Looking at a general Slater determinant

$$|\Phi_0\rangle = \hat{a}_i^\dagger \hat{a}_j^\dagger ... \hat{a}_n^\dagger \,|0\rangle \tag{3.63}$$

If this SD is the ground state of our system, we can use it as a reference state. We define the highest lying occupied state as the Fermi level, and name all states above the Fermi level *particle states* or *virtual states*. If a state below the Fermi level is vacant, we name it a *hole state*. From here on out, we will use a distinct naming pattern for indices. Indices using the latin alphabet using letters $i, j, k, l, ...$ are reserved for *hole states*. Latin letters $a, b, c, d, ...$ are reserved for *particle states*. Sometimes, we want to name more general states that can take the form of either a *hole state* or a *particle state*. We use the latin letters $p, q, r, s, ...$ For a more convenient way of writing, operators will be written on a shorter and more convenient form

$$\hat{a}_a = \hat{a} \quad \hat{a}_b^\dagger = \hat{b}^\dagger \quad \hat{a}_i^\dagger = \hat{i}^\dagger \quad ... \tag{3.64}$$

And so forth. The reference state will be written as

$$|\Phi_0\rangle = \hat{i}^\dagger \hat{j}^\dagger \hat{k}^\dagger ... \hat{n}^\dagger \,|\rangle = |ijk...n\rangle = |\rangle \tag{3.65}$$

And excitations will be written as

$$\text{Single Excitation:} \quad |\Phi_i^a\rangle = |ajk...n\rangle = \hat{i}\hat{a}^\dagger \,|\rangle \tag{3.66}$$

$$\text{Double Excitation:} \quad \left|\Phi_{ij}^{ab}\right\rangle = |abk...n\rangle = \hat{i}\hat{j}\hat{a}^\dagger \hat{b}^\dagger \,|\rangle \tag{3.67}$$

Where the use of annihilation operators for *hole states* no longer produce zero when used on the reference state. But simply remove one particle from the

reference state and create a *hole state*.

$$\hat{a}_i \left|\right\rangle = \left|\Phi_i\right\rangle = \left|jk...n\right\rangle \tag{3.68}$$

This will introduce a small change in Wick's theorem, as the only non-zero contractions are now

$$\overset{\frown}{\hat{i}^\dagger \hat{j}} = \delta_{ij} \tag{3.69}$$

And

$$\overset{\frown}{\hat{a}\hat{b}^\dagger} = \delta_{ab} \tag{3.70}$$

Contractions relative to the Fermi vacuum will now be denoted by brackets *above* the operators instead of below. Apart from this, Wick's theorem is unchanged relative to the Fermi vacuum.

A very important property of the reference state, is the expectation value for the hamiltonian.

$$\left\langle\right| \hat{H} \left|\right\rangle = \left\langle\Phi_0\right| \hat{H} \left|\Phi_0\right\rangle = \left\langle ijk...n\right| \hat{H} \left|ijk...n\right\rangle \tag{3.71}$$

We name this the reference Energy. The result is given by [3]

$$E_{\text{ref}} = \left\langle\Phi_0\right| \hat{H} \left|\Phi_0\right\rangle = \sum_i h_{ii} + \frac{1}{2} \sum_{ij} \left\langle ij||ij\right\rangle \tag{3.72}$$

3.8 Normal ordering of Operators

After defining the new vacuum, we will now rewrite the operators with respect to the reference state.

3.8.1 One-Body Operator

Consider a general one-body operator

$$\hat{F} = \sum_{pq} \left\langle p\right| \hat{f} \left|q\right\rangle \hat{p}^\dagger \hat{q} \tag{3.73}$$

Using Wick's theorem to rewrite the string of operators

$$\hat{p}^\dagger \hat{q} = \{\hat{p}^\dagger \hat{q}\} + \overset{\frown}{\hat{p}^\dagger \hat{q}} \tag{3.74}$$

We get

$$\hat{F} = \sum_{pq} \langle p| \hat{f} |q\rangle \{\hat{p}^\dagger \hat{q}\} + \sum_{i} \langle i| \hat{f} |i\rangle \tag{3.75}$$

$$= \hat{F}_N + \sum_{i} \langle i| \hat{f} |j\rangle \tag{3.76}$$

We notice that since

$$\langle\, |\hat{F}_N|\, \rangle = 0 \quad \rightarrow \quad \sum_{i} \langle i| \hat{f} |i\rangle = \langle\, |\hat{F}|\, \rangle \tag{3.77}$$

So we can rewrite the equation as

$$\hat{F} = F_N + \langle\, |\hat{F}|\, \rangle \tag{3.78}$$

Meaning that F_N represent the difference between $\hat{F}$ and the Fermi expectation value.

3.8.2 Two-Body operators

The general two-body operator given by

$$\hat{G} = \frac{1}{4} \sum_{pqrs} \langle pq|\hat{g}|rs\rangle_A \hat{p}^\dagger \hat{q}^\dagger \hat{s}\hat{r} \tag{3.79}$$

Although the method will be identical for a two-body operator as for a one-body operator, we will require a much larger sum over all possible contractions when using Wick's theorem. Calculation of the result can be viewed in [3].

$$\hat{G} = \frac{1}{4} \sum_{pqrs} \langle pq|\hat{g}|rs\rangle_A \{\hat{p}^\dagger \hat{q}^\dagger \hat{s}\hat{r}\} + \sum_{ipq} \langle pi|\hat{g}|qi\rangle_A \{\hat{p}^\dagger \hat{q}\} + \frac{1}{2} \sum_{ij} \langle ij|\hat{g}|ij\rangle_A \tag{3.80}$$

As for the one-body operator

$$\langle\, |\hat{G}|\, \rangle = \frac{1}{2} \sum_{ij} \langle ij|\hat{g}|ij\rangle_A \tag{3.81}$$

We can now name the terms

$$\hat{G} = \hat{G}_N + \hat{G}'_N + \langle\, |\hat{G}|\, \rangle \tag{3.82}$$

Where $\hat{G}'_N$ is a normal-ordered two-body operator.

3.9 Partitioning the Hamiltonian Operator

The Hamiltonian has been shown to consist of a one-body and a two-body term

$$\hat{H} = \hat{H}_1 + \hat{H}_2 \tag{3.83}$$

One can, however, write it in terms of a zero-order term and a perturbation

$$\hat{H} = \hat{H}_0 + \hat{V} \tag{3.84}$$

It is convenient to choose a zero-order Hamiltonian that is diagonal

$$\hat{H}_0 = \sum_p \epsilon_p \hat{p}^\dagger \hat{p} \tag{3.85}$$

This means we can write the perturbation as

$$\hat{V} = (\hat{H}_1 - \hat{H}_0) + \hat{H}_2 \tag{3.86}$$

$$= \sum_{pq} (h_{pq} - \epsilon_p \delta_{pq}) \hat{p}^\dagger \hat{q} + \frac{1}{4} \langle pq||rs\rangle \, \hat{p}^\dagger \hat{q}^\dagger \hat{s} \hat{r} \tag{3.87}$$

First, we define a Fock operator, $\hat{F}$, and a common practice is to choose the orbital energies as the diagonal elements of this Fock operator.

$$\hat{F} = \sum_{pq} f_{pq} \hat{p}^\dagger \hat{q} \tag{3.88}$$

With the matrix element defined as

$$f_{pq} = h_{pq} + u_{pq} \tag{3.89}$$

here u_{pq} is the matrix element of a one-body operator $\hat{U}$ implemented to simplify the zeroth-order term $\hat{H}_0$ and by simplifying the result when normal ordering the Hamiltonian later. See (3.110)

$$\hat{U} = \sum_{pq} u_{pq} \hat{p}^\dagger \hat{q} \tag{3.90}$$

$$u_{pq} = \sum_i \langle pi||qi\rangle \tag{3.91}$$

This means we can write $\hat{F} = \hat{H}_1 + \hat{U}$. Inserting the Fock operator into the perturbation

$$\hat{V} = \hat{F} - \hat{H}_0 - \hat{U} + \hat{H}_2 \tag{3.92}$$

$$= \sum_{pq}(f_{pq} - \epsilon_p\delta_{pq} - u_{pq})\hat{p}^\dagger\hat{q} + \frac{1}{4}\sum_{pqrs}\langle pq||rs\rangle\,\hat{p}^\dagger\hat{q}^\dagger\hat{s}\hat{r} \tag{3.93}$$

For a non-canonical Hartree-Fock case, the Fock matrix is diagonal, namely

$$f_{pq} = \epsilon_p\delta_{pq} \tag{3.94}$$

This means the perturbation can be rewritten as

$$\hat{V} = -\sum_{pq}u_{pq}\hat{p}^\dagger\hat{q} + \frac{1}{4}\sum_{pqrs}\langle pq||rs\rangle\,\hat{p}^\dagger\hat{q}^\dagger\hat{s}\hat{r} \tag{3.95}$$

With the zeroth-order energies given by

$$\hat{H}_0 = \sum_p \epsilon_p\hat{p}^\dagger\hat{p} \qquad \epsilon_p = h_{pp} + \sum_i\langle pi||pi\rangle \tag{3.96}$$

The noncanonical case, the Fock operator, $\hat{F}$, is block diagonal, with $f_{ia} = 0$. To, again, cancel out the single orbital energies from the perturbation, we split the Fock operator into a diagonal and off-diagonal term

$$\hat{F} = \hat{F}^d + \hat{F}^o \tag{3.97}$$

The diagonal term will now be canceled out, and we are left with the perturbation

$$\hat{V} = -\sum_{pq}(f^o_{pq} - u_{pq})\hat{p}^\dagger\hat{q} + \frac{1}{4}\sum_{pqrs}\langle pq||rs\rangle\,\hat{p}^\dagger\hat{q}^\dagger\hat{s}\hat{r} \tag{3.98}$$

For convience, we can organize the perturbation into a one-body part and a two-body part, $\hat{V}_1$ and $\hat{V}_2$

$$\hat{V}_1 = \hat{F}^o - \hat{U} = \sum_{pq}(f^o_{pq} - u_{pq})\hat{p}^\dagger\hat{q} \tag{3.99}$$

$$\hat{V}_2 = \hat{H}_2 = \frac{1}{4}\sum_{pqrs}\langle pq||rs\rangle\,\hat{p}^\dagger\hat{q}^\dagger\hat{s}\hat{r} \tag{3.100}$$

Resulting in the Hamiltonian

$$\hat{H} = \hat{H}_0 + \hat{V}_1 + \hat{V}_2 \tag{3.101}$$

3.10 Normal Ordering of Hamiltonian

To sum it all up, I will now present a normal ordering of the partitioned Hamiltonian operator. Starting by applying Wick's theorem to the zeroth order term

$$(\hat{H}_0)_N = \hat{H}_0 - E^{(0)} = \sum_p \epsilon_p \hat{p}^\dagger \hat{p} - \sum_i e_i = \sum_p \epsilon_p \{\hat{p}^\dagger \hat{p}\} \tag{3.102}$$

Then applying Wick's theorem to the one- and two-body perturbations given in (3.100)

$$\hat{V}_1 = (\hat{V}_1)_N + \langle\, |\hat{V}_1| \,\rangle \tag{3.103}$$

Where we have

$$(\hat{V}_1)_N = \hat{F}_N^o - \hat{U}_N = \sum_{pq} (f_{pq}^o - u_{pq}) \{\hat{p}^\dagger \hat{q}\} \tag{3.104}$$

and

$$\langle\, |\hat{V}_1| \,\rangle = -\sum_{ij} \langle ij||ij\rangle = -\langle\, |\hat{U}| \,\rangle \tag{3.105}$$

Turning to the two-body perturbation and using (3.80)

$$\hat{V}_2 = (\hat{V}_2)_N + \hat{V}_N' + \langle\, |\hat{V}_2| \,\rangle \tag{3.106}$$

Where we have the following

$$(\hat{V}_2)_N = \frac{1}{4} \sum_{pqrs} \langle pq||rs\rangle \, \{\hat{p}^\dagger \hat{q}^\dagger \hat{s} \hat{r}\} \tag{3.107}$$

$$V_N' = \sum_{pq} \langle pi||pi\rangle \, \{\hat{p}^\dagger \hat{q}\} \tag{3.108}$$

$$\langle\, |\hat{V}_2| \,\rangle = \frac{1}{2} \sum_{ij} \langle ij||ij\rangle \tag{3.109}$$

We notice now, that after normal ordering the operators, we are left with many terms that can be reorganized into zero-, one- and two-body parts. We can rewrite the total perturbation as

$$\hat{V} = \hat{F}_N^o - \hat{U}_N + \langle\, |\hat{V}_1| \,\rangle + (\hat{V}_2)_N + \hat{V}_N' + \langle\, |\hat{V}_2| \,\rangle \tag{3.110}$$

Now, by construction of $\hat{U}$, we see that $\hat{U}$ and $\hat{V}'_N$ cancel each other out. Renaming $(\hat{V}_2)_N = \hat{W}_N$ We see that the terms left can be written as

$$\hat{V} = \hat{F}^o_N + \hat{W}_N + \langle\, |\hat{V}|\, \rangle \tag{3.111}$$

By applying the same logic as earlier, we write

$$\hat{V}_N = \hat{V} - \langle\, |\hat{V}|\, \rangle \tag{3.112}$$

So that we finally can write the normal ordered perturbation as

$$\hat{V}_N = \hat{F}^o_N + \hat{W}_N \tag{3.113}$$

We notice here the use of the diagonal Fock matrix. This matrix is just zero in the canonical Hartree Fock case.

3.11 Correlation Energy

All the many-body quantum mechanics methods described in this thesis will aim to compute the correlation energy. We derive it by substracting

$$\langle\, |\hat{H}|\, \rangle = \langle\, |\hat{H}_0|\, \rangle + \langle\, |\hat{V}|\, \rangle \tag{3.114}$$

from the partitioned hamiltonian $\hat{H} = \hat{H}_0 + \hat{V}$. Resulting in

$$\hat{H} - \langle\, |\hat{H}|\, \rangle = \hat{H}_0 - \langle\, |\hat{H}_0|\, \rangle + \hat{V} - \langle\, |\hat{V}|\, \rangle \tag{3.115}$$

This can be rewritten in terms of normal ordered operators as

$$\hat{H}_N = (\hat{H}_0)_N + \hat{V}_N \tag{3.116}$$

The Schrdinger equation for this operator is given as

$$\hat{H}_N \Psi = \Delta E \Psi \tag{3.117}$$

Where we have defined the computed energy as

$$\Delta E = E - E_{\text{ref}} \tag{3.118}$$

or

$$E = E_{\text{ref}} + \Delta E \tag{3.119}$$

This energy is named the correlation energy, and the goal of my thesis has been to implement and compare different methods to compute this energy for different

systems. The reference energy, given as

$$E_{\text{ref}} = \langle\, |\hat{H}_0|\, \rangle + \langle\, |\hat{V}|\, \rangle \tag{3.120}$$

Is easily computed when the basis is set up. Finally, we can set up the fully partitioned normal ordered Hamiltonian as

$$\hat{H}_N = \hat{F}_N^d + \hat{F}_N^o + \hat{W}_N \tag{3.121}$$

Chapter 4

Diagramatic Representation

It can be quite cumbersome and error-prone to treat the manipulation of states and operators with second quantization [3]. The soon to be introduced many body methods will include various sums over states. One can introduce a new formalism originated in quantum field theory in the form of Feynman diagrams to depict and list these sums. It is quite common to refer to these sums simply as *diagrams*. The main benefits of the diagramatic notation include an easy way of listing non vanishing terms and elucidating various cancelations in the sums.

4.1 The Slater Determinant

We begin, as in second quantization, by setting up the Slater determinant. There is a time dependent direction on the diagrams going up. The actual times are irrelevant, but the sequence is important. The reference state, $|\,\rangle = |\Phi\rangle$ is depicted simply as a horizontal line

---

Figure 4.1: Diagram for the reference state $|\,\rangle$

While the hole states are represented by vertical lines either going up or down, particle and hole states are depicted by a vertical line. An arrow pointing up relates a particle state, while an arrow pointing down will mean a hole state. Depicting the two states $|\Phi^a\rangle$ and $|\Phi_i\rangle$

Figure 4.2: Diagrams for the addition of a particle and a hole state, $|\Phi^a\rangle$ and $|\Phi_i\rangle$ respectively

The ket-variant of the singly excited Slater determinant $\langle\Phi_i^a|$ can be drawn as

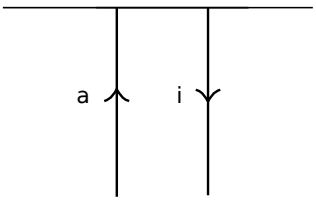

Figure 4.3: Diagram for the singly excited ket state $\langle\Phi_i^a|$

And the doubly excited states $\left|\Phi_{ij}^{ab}\right\rangle$ can be drawn as

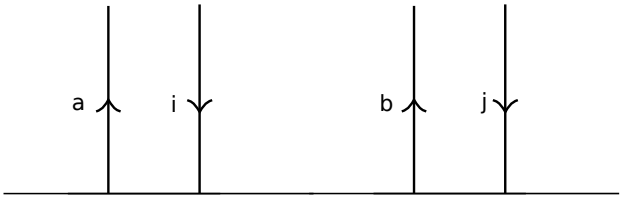

Figure 4.4: Diagram for the doubly excited bra state $\left|\Phi_{ij}^{ab}\right\rangle$

4.2 Operators

We need a convention for one body operators as well. The one body Hamiltonian operator is given by

$$\hat{H}_1 = \sum_{pq} \langle p|h|\rangle \, \hat{p}^\dagger \hat{q} \tag{4.1}$$

We will represent the matrix element $\langle p|h|\rangle$ by a dashed line, while there will be one line entering and one line leaving the operator due to the annihilation and creation operator. Because the operator behaves different depending on wether the general operators p and q are hole or particle states, the one body operator will I list the four normal ordered one body operators below [3]

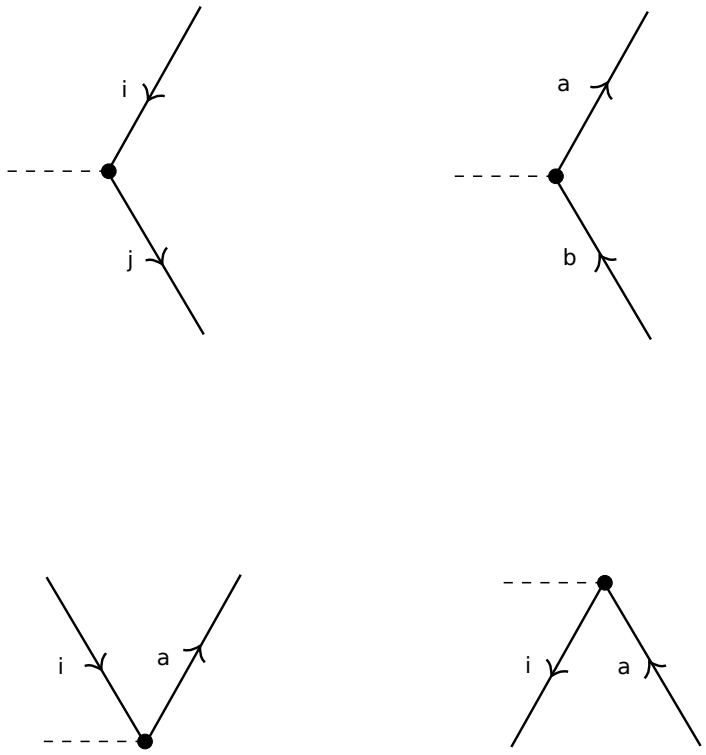

Figure 4.5: Diagrams for four different variants of the one body operator. From left to right, the operators shown are $\sum_{ij} h_{ij} i^\dagger j$, $\sum_{ab} h_{ab} a^\dagger b$, $\sum_{ai} h_{ai} a^\dagger i$ and $\sum_{ai} h_{ia} i^\dagger a$

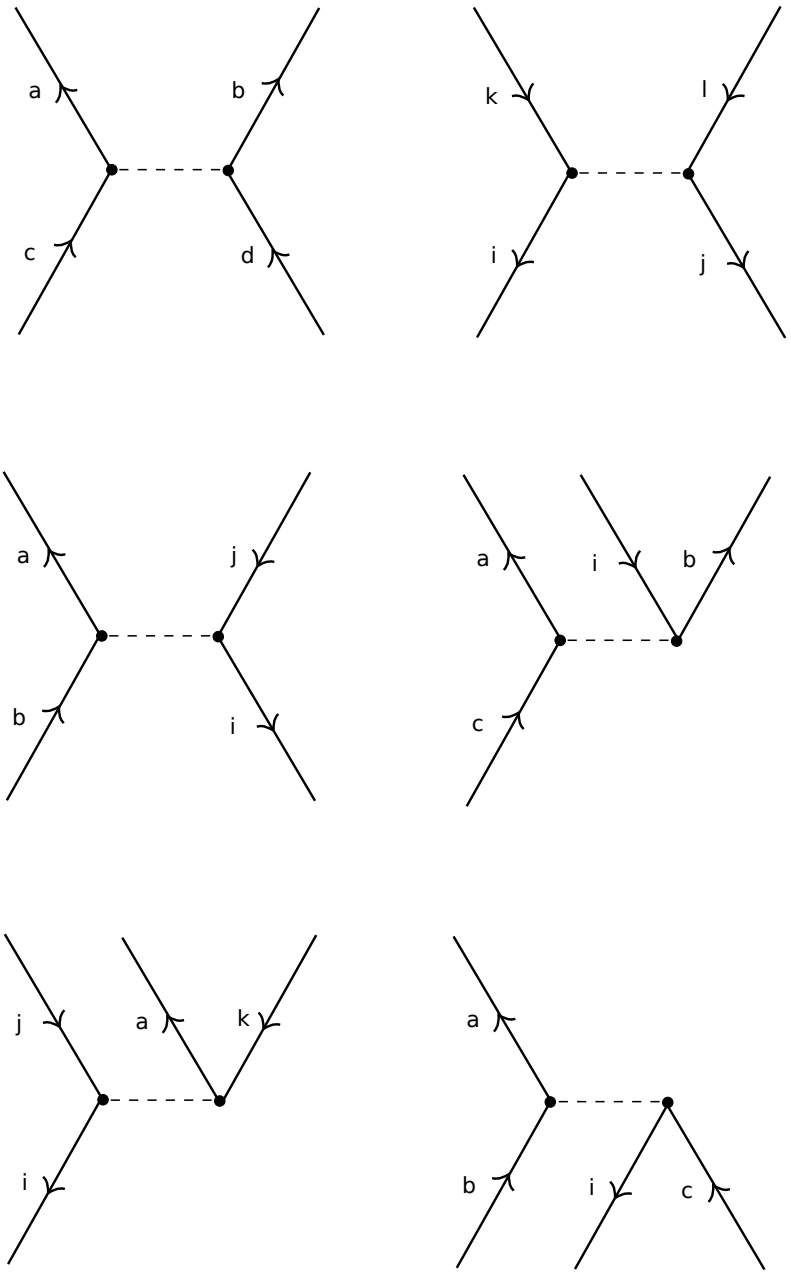

Figure 4.6: Diagrams for four different variants of the one body operator. From left to right, the operators shown are $\sum_{ij} h_{ij} i^\dagger j$, $\sum_{ab} h_{ab} a^\dagger b$, $\sum_{ai} h_{ai} a^\dagger i$ and $\sum_{ai} h_{ia} i^\dagger a$

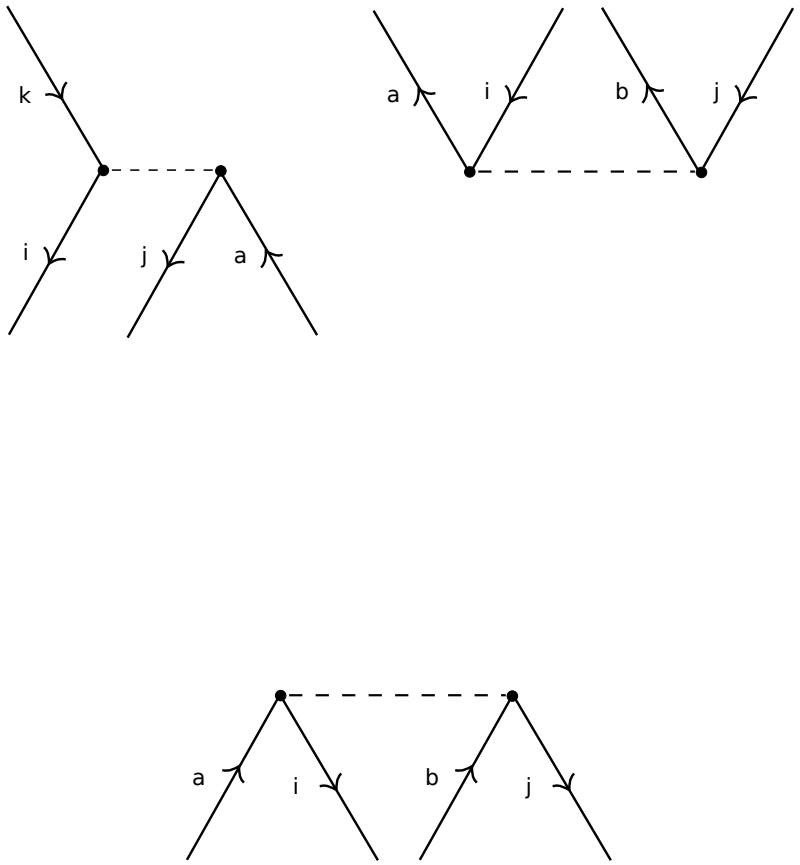

Figure 4.7: Diagrams for four different variants of the one body operator. From left to right, the operators shown are $\sum_{ij} h_{ij} i^\dagger j$, $\sum_{ab} h_{ab} a^\dagger b$, $\sum_{ai} h_{ai} a^\dagger i$ and $\sum_{ai} h_{ia} i^\dagger a$

4.3 Contractions and Inner products

As seen, contractions are an important part of many body methods. Representing contractions is easy with using a diagrammatic approach. It is done by connecting the lines between operators and Slater determinants. Take, as an example, the Slater determinant [2, 3]

$$|\Phi_i^a\rangle = \hat{a}^\dagger \hat{i}| \,\rangle \tag{4.2}$$

and the general one body operator

$$\hat{U} = \sum_{bc} \langle b|\hat{u}|c\rangle \, \{\hat{b}^\dagger \hat{c}\} \tag{4.3}$$

When the operator $\hat{U}$ acts on the Slater determinant, we the resulting Slater determinant will change

$$\hat{U} \, |\Phi_i^a\rangle = \sum_{bc} \langle b|\hat{u}|c\rangle \, \{\hat{b}^\dagger \hat{c}\}\{\hat{a}^\dagger \hat{i}\}| \,\rangle \tag{4.4}$$

We can write this out using the generalized Wick's theorem, noticing that there only one possible contraction that is non-zero.

$$= \langle b|\hat{u}|c\rangle \, \{\hat{b}^\dagger \hat{c} \hat{a}^\dagger \hat{i}\} + \langle b|\hat{u}|c\rangle \, \{\hat{b}^\dagger \overbrace{\hat{c}\hat{a}^\dagger} \hat{i}\} = 0 + \langle b|\hat{u}|c\rangle \, \delta_{ac} \left|\Phi_i^b\right\rangle \tag{4.5}$$

Which gives

$$\langle b|\hat{u}|a\rangle \, \{\hat{b}^\dagger \hat{i}\}| \,\rangle = \langle b|\hat{u}|a\rangle \left|\Phi_i^b\right\rangle \tag{4.6}$$

The diagrammatic representation will be shown as

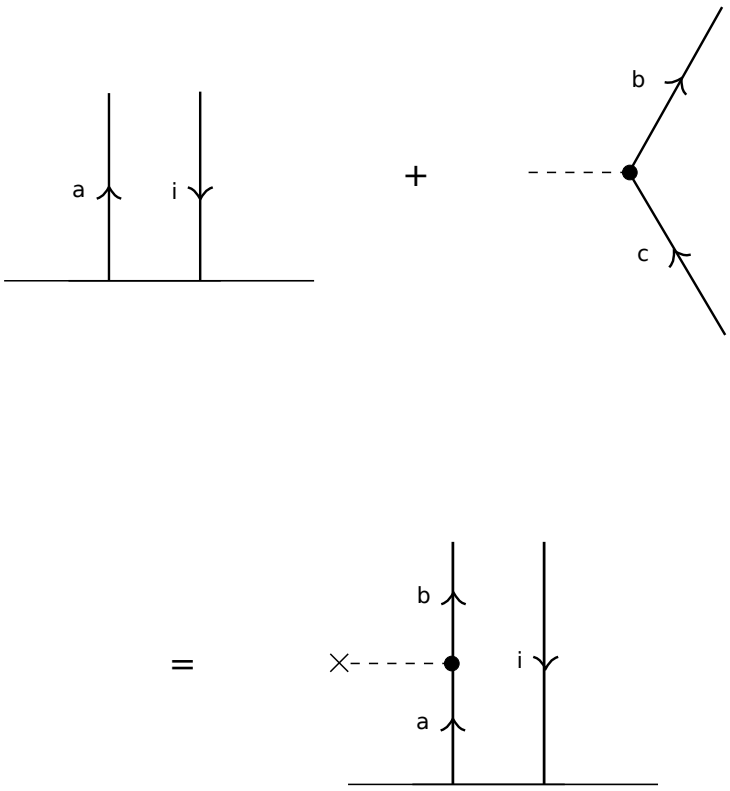

Figure 4.8: Diagrams for four different variants of the one body operator. From left to right, the operators shown are $\sum_{ij} h_{ij} i^\dagger j$, $\sum_{ab} h_{ab} a^\dagger b$, $\sum_{ai} h_{ai} a^\dagger i$ and $\sum_{ai} h_{ia} i^\dagger a$

Representing an inner product of two Slater Determinants is done by putting together the diagram for a ket state and the diagram for a bra state. Looking at the previous example, taking the expectation value of the general operator $\hat{U}$, we get

$$\left\langle \Phi_k^d \right| \hat{U} \left| \Phi_i^a \right\rangle \tag{4.7}$$

Which can be written out as

$$\sum_{bj} \langle b|\hat{u}|c\rangle \, \langle \, |\{\hat{k}^\dagger \hat{d}\}\{\hat{b}^\dagger \hat{c}\}\{\hat{a}^\dagger \hat{i}\}| \, \rangle \tag{4.8}$$

Calculating with generalized Wick's theorem

$$= \langle d|\hat{u}|a\rangle \, \delta_{db}\delta_{ac}\delta_{ki} \tag{4.9}$$

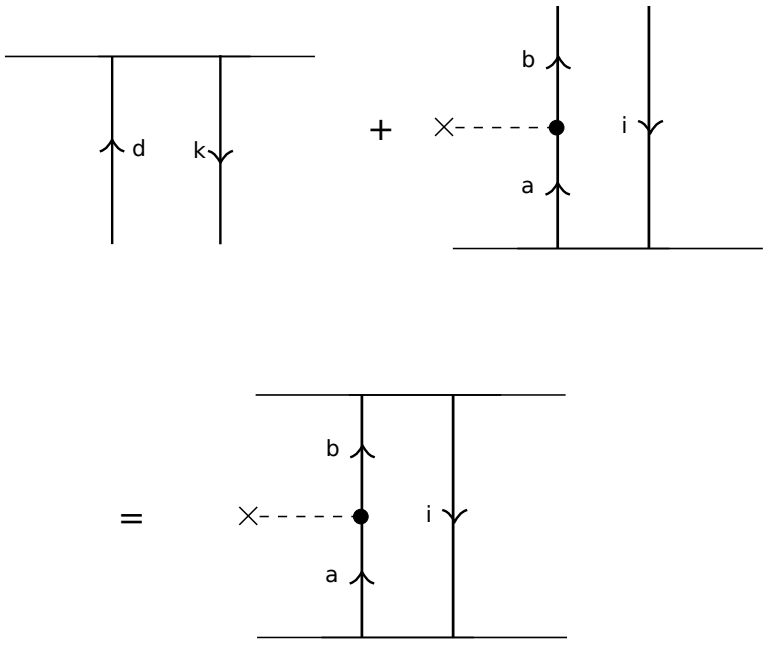

Figure 4.9: Diagrams for four different variants of the one body operator. From left to right, the operators shown are $\sum_{ij} h_{ij} i^\dagger j$, $\sum_{ab} h_{ab} a^\dagger b$, $\sum_{ai} h_{ai} a^\dagger i$ and $\sum_{ai} h_{ia} i^\dagger a$

4.4 Interpreting Diagrams

Diagrams can be translated back to mathematical expressions using a toolset for interpreting diagrams. The most common use of diagrams is to present different

4.5 Linked Diagram theorem

Chapter 5

Many-Body Methods

We define an ansatz for the ground state, $|\Phi_0\rangle$ as a Slater determinant consisting of the single particle states, $|\phi_i\rangle$

$$|\Psi\rangle \approx |\Phi_0\rangle = \frac{1}{\sqrt{N!}} \begin{vmatrix} \phi_1(\mathbf{x}_1) & \phi_2(\mathbf{x}_1) & ... & \phi_N(\mathbf{x}_1) \\ \phi_1(\mathbf{x}_2) & \phi_2(\mathbf{x}_2) & ... & \phi_N(\mathbf{x}_2) \\ ... & & & \\ \phi_1(\mathbf{x}_N) & \phi_2(\mathbf{x}_N) & ... & \phi_N(\mathbf{x}_N) \end{vmatrix} \tag{5.1}$$

Written in terms of second quantization

$$|\Phi_0\rangle = \left(\prod_{i \leq F} \hat{i}^\dagger \right) |0\rangle = |\ \rangle \tag{5.2}$$

Typically one chooses well-known and mathematically simple single particle states that are easy to implement. In this thesis, I have used a free particle wave function as single-particle states for infinite matter. Using this basis, I obviously fail to incorporate the interaction between electrons since ϕ_1 remains unchanged if I also add ϕ_2. This can be solved by using a smarter basis, which is the goal of Hartree-Fock. Hartree-Fock will, through an iterative method, change the single particle states to get a better result. This can be viewed as incorporating the interaction as a *mean field* approximation.

I will in this thesis present, and use, three *post Hartree-Fock* methods. These are *Full Configuration Interaction Theory*, *Many Body Perturbation Theory* and *Coupled Cluster Theory*, where the latter is the main focus of my thesis. These methods aim to compute the *Corrolation Energy* as presented in the chapter on Second Quantization. It is quite common to first implement the Hartree-Fock method, providing the most precise reference energy.

5.1 Full Configuration Interaction Theory

The first *Post Hartree-Fock* method to be presented is the *Full Configuration Interaction theory*. We expand the true wave function as a linear combination of the ground state ansatz and all possible excitations

$$|\Psi\rangle = C_0 |\Phi_0\rangle + \sum_{ai} C_i^a |\Phi_i^a\rangle + \sum_{abij} C_{ij}^{ab} \left|\Phi_{ij}^{ab}\right\rangle + ... \tag{5.3}$$

Which can be rewritten in terms of a *correlation operator*

$$|\Psi\rangle = (C_0 + \hat{C}) |\Phi_0\rangle \tag{5.4}$$

With

$$\hat{C} = \sum_{ai} C_i^a \hat{a}^\dagger \hat{i} + \sum_{abij} C_{ij}^{ab} \hat{a}^\dagger \hat{b}^\dagger \hat{j} \hat{i} + ... \tag{5.5}$$

We can name the terms such that

$$\hat{C} = \hat{C}_1 + \hat{C}_2 + ... \tag{5.6}$$

We use intermediate normalization, which set $C_0 = 1$, such that we get the relation

$$\langle \Psi | \Phi_0 \rangle = C_0 \langle \Phi_0 | \Phi_0 \rangle = 1 \tag{5.7}$$

We can now rewrite $|\Psi\rangle$

$$|\Psi\rangle = (1 + \hat{C}) |\Phi_0\rangle \tag{5.8}$$

To simplify the notation, we can write the equation in terms of P and H, which symbolizes all possible chains of creation and annihilation operators

$$|\Psi\rangle = \sum_{PH} C_H^P \left|\Phi_H^P\right\rangle = \left(\sum_{PH} C_H^P \hat{A}_H^P \right) |\Phi_0\rangle \tag{5.9}$$

We are working with orthonormal states, meaning that

$$\langle \Psi | \Psi \rangle = \sum_{PH} \left| C_H^P \right|^2 = 1 \tag{5.10}$$

The only thing left now, is defining how to compute the correlation energy. We write the expression for the energy as

$$E = \langle \Psi|\hat{H}|\Psi \rangle = \sum_{PHP'H'} (C_H^P)^* \langle \Phi_H^P|\hat{H}|\Phi_{H'}^{P'} \rangle C_{H'}^{P'} \tag{5.11}$$

5.1.1 The Hamiltonian Matrix

We can build a Hamiltonian matrix consisting of all possible combinations of Slater determinants, i.e. all possible combinations of P, H and P', H'. The matrix elements will be the expectation value for the Hamiltonian with respect to the given Slater determinants.

$$\hat{\mathcal{H}} = \begin{pmatrix} & 0p-0h & 1p-1h & 2p-2h & 3p-3h & 4p-4h & ... & Np-Nh \\ 0p-0h & x & x & x & 0 & 0 & 0 & 0 \\ 1p-1h & x & x & x & x & 0 & 0 & 0 \\ 2p-2h & x & x & x & x & x & & 0 \\ 3p-3h & 0 & x & x & x & x & & 0 \\ 4p-4h & 0 & 0 & x & x & x & & 0 \\ ... & 0 & 0 & & & & & \\ Np-Nh & 0 & 0 & 0 & 0 & 0 & & x \end{pmatrix} \tag{5.12}$$

Above is an example of a general Hamiltonian matrix, $\mathcal{H}$, set up for a N-particles, N-holes, basis. One can notice that many matrix elements are zero. This is because the Hamiltonian only have a two-particle interaction term. If we have performed Hartree-Fock calculations, or start out with a Hartree-Fock basis, we have shifted the basis such that all matrix elements of the type

$$\Big\langle 0p-0h|\hat{H}|1p-1h\Big\rangle = \Big\langle 1p-1h|\hat{H}|0p-0h\Big\rangle = 0 \tag{5.13}$$

Giving us a shifted Hamiltonian matrix

$$\hat{\mathcal{H}} = \begin{pmatrix} & 0p-0h & 1p-1h & 2p-2h & 3p-3h & 4p-4h & ... & Np-Nh \\ 0p-0h & \tilde{x} & 0 & \tilde{x} & 0 & 0 & 0 & 0 \\ 1p-1h & 0 & \tilde{x} & \tilde{x} & \tilde{x} & 0 & 0 & 0 \\ 2p-2h & \tilde{x} & \tilde{x} & \tilde{x} & \tilde{x} & \tilde{x} & & 0 \\ 3p-3h & 0 & \tilde{x} & \tilde{x} & \tilde{x} & \tilde{x} & & 0 \\ 4p-4h & 0 & 0 & \tilde{x} & \tilde{x} & \tilde{x} & & 0 \\ ... & 0 & 0 & & & & & \\ Np-Nh & 0 & 0 & 0 & 0 & 0 & & \tilde{x} \end{pmatrix} \tag{5.14}$$

To find the ground state correlation energy, the normal procedure is to diagonalize the Hamiltonian matrix through computational algorithms. If we have a finite size Hilbert space, we can set up a finite Hamiltonian matrix which, when diagonalized, will provide us with the exact ground state correlation energy.

Unfortunatly, the Full Configuration Interaction Theory is very computationally costly. The Hamiltonian matrix will grow exponentially fast for large Hilbert spaces, which both increases the memory usage dramatically and increases the prosessing power associated with diagonalizing the matrix. For infinite and very large Hilbert spaces, one can truncate the number of excitations at some level to reduce the size of Hamiltonian matrix. I will later refer to this as just *Configuration Interaction theory*.

5.1.2 Computational cost

As a brief example on how costly the full configuration interaction theory can be, we look at the nucleus of an oxygen atom. For a system consisting of N states and n particles, the total number of unique Slater determinants is given by [20]

$$\binom{N}{n} = \frac{n!}{(n-N)!N!} \tag{5.15}$$

Looking at the Oxygen nucleus, we have 8 protons and 8 neutrons. If we only include the first major shells, 0s, 0p, 1s0d and 1p0f, we have a total of 40 states the neutrons and protons can occupy. Using (5.15)

$$\binom{40}{8} = \frac{40!}{32!8!} \approx 10^9 \tag{5.16}$$

for both the protons and the neutrons. Multiplying them together, we get

$$10^9 10^9 = 10^{18} \tag{5.17}$$

Slater determinants for the whole system. This shows how fast the dimensionality explodes!

5.2 Many-body Perturbation Theory

The Perturbation theory presents a non-iterative approach to approximating the ground state energy. The approach is similar to previous methods. We start by splitting the Hamiltonian into a solvable part and a perturbation.

$$\hat{H} = \hat{H}_0 + \hat{V} \tag{5.18}$$

Where we have chosen our basis such that

$$\hat{H}_0 |\Psi_0\rangle = W_0 |\Psi_0\rangle \tag{5.19}$$

We split the basis aswell

$$|\Psi_0\rangle = |\Phi_0\rangle + \sum_i^\infty c_i |\phi_i\rangle \tag{5.20}$$

Assuming intermediate normalization

$$\langle\Phi_0|\Psi_0\rangle = 1 \tag{5.21}$$

We can calculate the total exact energy

$$E = \langle\Phi_0| \hat{H}_0 |\Psi_0\rangle + \langle\Phi_0| \hat{V} |\Psi_0\rangle \tag{5.22}$$

Where we know that

$$\langle\Phi_0| \hat{H}_0 |\Psi_0\rangle = W_0 \tag{5.23}$$

And we get the corrolation energy

$$E - W_0 = \Delta E = \langle\Phi_0| \hat{V} |\Psi_0\rangle \tag{5.24}$$

We will usually aim to compute this energy when doing MBPT.

5.2.1 General derivation of Many Body Particle Theory equations

Looking at the equation

$$\hat{V} |\Psi_0\rangle = \hat{H} |\Psi_0\rangle + \hat{H}_0 |\Psi_0\rangle \tag{5.25}$$

We reorganize and add the term $\omega |\Psi_0\rangle$ on both sides

$$\hat{V} |\Psi_0\rangle + \omega |\Psi_0\rangle - \hat{H} |\Psi_0\rangle = \omega |\Psi_0\rangle - \hat{H}_0 |\Psi_0\rangle \tag{5.26}$$

Remembering that $\hat{H} |\Psi_0\rangle = E |\Psi_0\rangle$, we get

$$|\Psi_0\rangle = \frac{\hat{V} + \omega - E}{\omega - \hat{H}_0} |\Psi_0\rangle \tag{5.27}$$

Before continuing, we introduce the operators $\hat{P}$ and $\hat{Q}$, such that

$$|\Psi_0\rangle = \hat{P}\,|\Psi_0\rangle + \hat{Q}\,|\Psi_0\rangle = |\Phi_0\rangle\,\langle\Phi_0|\Psi_0\rangle + \sum_i |\Phi_i\rangle\,\langle\Phi_i|\Psi_0\rangle \tag{5.28}$$

$$= |\Phi_0\rangle + \chi \tag{5.29}$$

Giving

$$|\Phi_0\rangle = \hat{P}\,|\Psi_0\rangle \qquad \chi = \hat{Q}\,|\Psi_0\rangle \tag{5.30}$$

Using $\hat{R}(\omega) = \frac{\hat{Q}}{\left(\omega - \hat{H}_0\right)}$ and multiplying both sides with $\hat{Q}$ from the left in equation (5.27) we attain

$$\hat{Q}\,|\Psi_0\rangle = \hat{R}(\omega)\left(\hat{V} + \omega - E\right)|\Psi_0\rangle \tag{5.31}$$

Using equations (5.28) and (5.30), we get

$$|\Psi_0\rangle = |\Phi_0\rangle + \hat{R}(\omega)\left(\hat{V} + \omega - E\right)|\Psi_0\rangle \tag{5.32}$$

This is an iterative scheme. We can substitute $|\Psi_0\rangle$ on the right hand side with the entire right hand side. This results in an infinite sum provided the series converges

$$|\Psi_0\rangle = \sum_0^\infty \left\{\hat{R}(\omega)(\hat{V} + \omega - E)\right\}^m |\Phi_0\rangle \tag{5.33}$$

The right hand side does include the energy, E, which must be computed using $E = W_0 + \Delta E$, and

$$\Delta E = \langle\Phi_0|\,\hat{V}\,|\Psi_0\rangle = \sum_0^\infty \langle\Phi_0|\,\hat{V}\left[\hat{R}(\omega)(\hat{V} - E + \omega)\right]^m |\Phi_0\rangle \tag{5.34}$$

5.2.2 Equations for Reileigh-Schrodinger Perturbation Theory

We can interpret ω different ways. I here present the Reileigh-Schrodinger Perturbation Theory which postulates that

$$\omega = E_0^{(0)} \tag{5.35}$$

Such that we get the expression for the resolvent

$$\hat{R}_0 = \frac{\hat{Q}}{E_0^0 - \hat{H}_0} \tag{5.36}$$

Giving

$$|\Psi_0\rangle = \frac{\hat{V} - \Delta E}{\omega - \hat{H}_0} |\Psi_0\rangle \tag{5.37}$$

and we get the final equation for the wave function

$$|\Psi_0\rangle = \sum_0^\infty \left\{ \hat{R}(\omega)(\hat{V} + -\Delta E) \right\}^m |\Phi_0\rangle \tag{5.38}$$

and for the correlation energy

$$\Delta E = \sum_0^\infty \langle \Phi_0 | \hat{V} \left[\hat{R}(\omega)(\hat{V} - \Delta E) \right]^m |\Phi_0\rangle \tag{5.39}$$

Taking a closer look at the energy-equations, we find that we can write the first orders as

$$\begin{aligned}
E^{(1)} &= \langle \Phi_0 | \hat{V} | \Phi_0 \rangle = V_{00} \\
E^{(2)} &= \langle \Phi_0 | \hat{V} \hat{R}_0 \hat{V} | \Phi_0 \rangle \\
E^{(3)} &= \langle \Phi_0 | \hat{V} \hat{R}_0 (\hat{V} - E^{(1)}) \hat{R}_0 \hat{V} | \Phi_0 \rangle \\
E^{(4)} &= \langle \Phi_0 | \hat{V} \hat{R}_0 (\hat{V} - E^{(1)}) \hat{R}_0 (\hat{V} - E^{(1)}) \hat{R}_0 \hat{V} | \Phi_0 \rangle - E^{(2)} \langle \Phi_0 | \hat{V} \hat{R}_0^2 \hat{V} | \Phi_0 \rangle
\end{aligned}$$

Because of the frequent appearance, we can rewrite $\hat{V} - E^{(1)}$ as

$$\hat{\Omega} = \hat{V} - E^{(1)} = \hat{V} - \langle \Phi_0 | \hat{V} | \Phi_0 \rangle \tag{5.40}$$

We name this new variable the wave operator, and rewrite the equations in a simpler form.

$$\begin{aligned}
E^{(1)} &= \langle \Phi_0 | \hat{V} | \Phi_0 \rangle = V_{00} \\
E^{(2)} &= \langle \Phi_0 | \hat{V} \hat{R}_0 \hat{V} | \Phi_0 \rangle \\
E^{(3)} &= \langle \Phi_0 | \hat{V} \hat{R}_0 \hat{\Omega} \hat{R}_0 \hat{V} | \Phi_0 \rangle \\
E^{(4)} &= \langle \Phi_0 | \hat{V} \hat{R}_0 \hat{\Omega} \hat{R}_0 \hat{\Omega} \hat{R}_0 \hat{V} | \Phi_0 \rangle - E^{(2)} \langle \Phi_0 | \hat{V} \hat{R}_0^2 \hat{V} | \Phi_0 \rangle
\end{aligned}$$

I am, in this thesis, concerned with calculating the correlation energy, and these four equations will be implemented for the Pairing model.

5.3 Hartree-Fock calculations

When doing Hartree-Fock calculation, we do a change of basis and instead of expanding our Hamiltonian, we vary the wavefunction to minimize the energy. We name the original basis by greek letters and the new basis by latin letters. The original basis should be chosen such that we can calculate the its expectation value.

$$\langle \Phi_0 | \hat{H} | \Phi_0 \rangle = E^{\mathrm{HF}} \tag{5.41}$$

Variational principle ensures that

$$E^{\mathrm{HF}} > 0 \tag{5.42}$$

We now introduce a change of basis

$$|\psi_a\rangle = \sum_{\lambda} C_{a\lambda} |\psi_\lambda\rangle \tag{5.43}$$

Varying $C_{p\lambda}$, we can look for the basis providing the lowest energy. We start by rewriting E^{HF} as a functional

$$E[\psi] = \sum_{a=1}^{N} \langle a | h | a \rangle + \frac{1}{2} \sum_{ab}^{N} \langle ab | v | ab \rangle \tag{5.44}$$

In terms of the original greek basis

$$E[\psi] = \sum_{a=1}^{N} \sum_{\alpha\beta} C^*_{a\alpha} C_{a\beta} \langle \alpha | h | \beta \rangle + \frac{1}{2} \sum_{ab}^{N} \sum_{\alpha\beta\gamma\delta} C^*_{a\alpha} C^*_{b\beta} C_{a\gamma} C_{b\delta} \langle \alpha\beta | v | \gamma\delta \rangle \tag{5.45}$$

To find the minima, we introduce a Lagrange multiplier before differentiating with respect to $C^*_{a\alpha}$. This will give N equations, one for each state, a. The equations are given by

$$\sum_{\beta} C_{a\beta} \langle \alpha | h | \beta \rangle + \sum_{b}^{N} \sum_{\beta\gamma\delta} C^*_{b\beta} C_{b\delta} C_{a\gamma} \langle \alpha\beta | v | \gamma\delta \rangle = \epsilon_a C_{a\alpha} \tag{5.46}$$

Defining

$$h^{\mathrm{HF}}_{\alpha\gamma} = \langle \alpha | h | \gamma \rangle + \sum_{b=1}^{N} \sum_{\beta\delta} C^*_{b\beta} C_{b\delta} \langle \alpha\beta | v | \gamma\delta \rangle \tag{5.47}$$

We get the short hand iterative equations to be solved

$$\sum_{\gamma} h^{\mathrm{HF}}_{\alpha\gamma} C_{a\gamma} = \epsilon_a C_{a\alpha} \tag{5.48}$$

Chapter 6

Coupled-Cluster Theory

In Coupled Cluster theory, the ansatz we make is to make an expansion in the wave function

$$|\Psi\rangle \approx e^{\hat{T}} |\Psi_0\rangle \tag{6.1}$$

The operator $\hat{T}$ is a linear combination of the cluster operators

$$\hat{T} = \hat{T}_1 + \hat{T}_2 + \hat{T}_3 + ... + \hat{T}_N \tag{6.2}$$

Where the operators represent

$$T_1 = \sum_{ia} t_i^a \hat{a}_a^\dagger \hat{a}_i \tag{6.3}$$

$$T_2 = \frac{1}{2} \sum_{ijab} t_{ij}^{ab} \hat{a}_a^\dagger \hat{a}_b^\dagger \hat{a}_j \hat{a}_i \tag{6.4}$$

$$T_2 = \left(\frac{1}{n!}\right)^2 \sum_{ij..ab..}^{n} t_{ij..n}^{ab..n} \hat{a}_a^\dagger \hat{a}_b^\dagger ... \hat{a}_n^\dagger \hat{a}_n ... \hat{a}_j \hat{a}_i \tag{6.5}$$

$$\tag{6.6}$$

We can write the configuration interaction wavefunction as

$$|\Psi_{CI}\rangle = (1 + \hat{C}) |\Phi_0\rangle \tag{6.7}$$

$$\hat{C} = \hat{C}_1 + \hat{C}_2 + ... = \sum_{ia} c_i^a a_a^\dagger a_i + \frac{1}{4} \sum_{ijab} c_{ij}^{ab} a_a^\dagger a_b^\dagger a_j a_i + ... \tag{6.8}$$

Comparing this linear expansion to the exponential expansion from Coupled Clus-

ter, we can see that

$$\hat{C}_2 = \hat{T}_2 + \frac{1}{2}T_1^2 \tag{6.9}$$

Where we can see that even if we truncate Configuration Interaction and Coupled Cluster at the same level, there are more *disconnected* wave function contributions (REFERENCE page 17 IN C&S) in the Coupled Cluster theory. Both the Coupled Cluster and Configuration Interaction theory provides the exact energy by including the operators to infinite order, i.e. no truncation.

6.1 Size Extensivity

It can be important to have a wave function that scales with size. Imagine a two particles, X and Y with infinity separation, they do not interact. This means we should be able to write the total energy as

$$E = E_X + E_Y \tag{6.10}$$

Doing Coupled Cluster

$$\hat{T} = \hat{T}_X + \hat{T}_Y \tag{6.11}$$

$$|\Psi\rangle_{CC} = e^{\hat{T}_X + \hat{T}_Y} |\Phi_0\rangle = e^{\hat{T}_X} e^{\hat{T}_Y} |\Psi_0\rangle \tag{6.12}$$

Since we can write the reference state as a product of the two seperated parts, we are able to write

$$E_{CC} = E_{CC}^X + E_{CC}^Y \tag{6.13}$$

This means Coupled Cluster is size extensive, contrary to the Configuration Interaction.

6.2 The CCD Equations

The Coupled Cluster Doubles equations can be finalized as

$$E_{CCD} = E_{ref} + \Delta E_{CCD} \tag{6.14}$$

With the reference energy defined as

$$E_{ref} = \sum_i \left\langle i \middle| \hat{h}_0 \middle| j \right\rangle + \sum_{ij} \langle ij|\hat{v}|ij\rangle + \frac{1}{2} A v_0 \tag{6.15}$$

and the corrolation energy given by

$$\Delta E_{CCD} = \frac{1}{4} \sum_{ijab} \langle ij|\hat{v}|ab\rangle \, t_{ij}^{ab} \tag{6.16}$$

v_0 is a constant, nonzero for the finite electron gas. After several applications of Wick's theorem, the amplitude equations can be reduced to

$$(\epsilon_i + \epsilon_j - \epsilon_a - \epsilon_b) t_{ij}^{ab} = \langle ab|\hat{v}|ij\rangle + \frac{1}{2} \sum_{cd} \langle ab|\hat{v}|cd\rangle \, t_{ij}^{cd} \tag{6.17}$$

$$+ \frac{1}{2} \sum_{kl} \langle kl|\hat{v}|ij\rangle \, t_{kl}^{ab} + \hat{P}\,(ij|ab) \sum_{kc} \langle kb|\hat{v}|cj\rangle \, t_{ik}^{ac} \tag{6.18}$$

$$+ \frac{1}{4} \sum_{klcd} \langle kl|\hat{v}|cd\rangle \, t_{ij}^{cd} t_{kl}^{ab} + \frac{1}{2} \hat{P}\,(ij|ab) \sum_{klcd} \langle kl|\hat{v}|cd\rangle \, t_{ik}^{ac} t_{lj}^{db} \tag{6.19}$$

$$- \frac{1}{2} \hat{P}(ij) \sum_{klcd} \langle kl|\hat{v}|cd\rangle \, t_{ik}^{ab} t_{jl}^{cd} - \frac{1}{2} \hat{P}(ab) \sum_{klcd} \langle kl|\hat{v}|cd\rangle \, t_{kl}^{bd} t_{ij}^{ac} \tag{6.20}$$

Where we have defined

$$\hat{P}(ij) = 1 - \hat{P}_{ij} \tag{6.21}$$

Where $\hat{P}_{ij}$ interchanges the two particles occupying the quantum states i and j. Furthermore, we define the operator

$$\hat{P}\,(ij|ab) = (1 - \hat{P}_{ij})(1 - \hat{P}_{ab}) \tag{6.22}$$

We notice that some parts are linear in the amplitude, while some are quadradic. Sorting them into the linear and quadradic parts, L and Q respectably, I get

$$L(t_{ij}^{ab}) = \frac{1}{2} \sum_{cd} \langle ab|\hat{v}|cd\rangle \, t_{ij}^{cd} + \frac{1}{2} \sum_{kl} \langle kl|\hat{v}|ij\rangle \, t_{kl}^{ab} + \hat{P}\,(ij|ab) \sum_{kc} \langle kb|\hat{v}|cj\rangle \, t_{ik}^{ac} \tag{6.23}$$

and

$$Q(t_{ij}^{ab}t_{ij}^{ab}) = \frac{1}{4}\sum_{klcd}\langle kl|\hat{v}|cd\rangle\, t_{ij}^{cd}t_{kl}^{ab} + \frac{1}{2}\hat{P}\,(ij|ab)\sum_{klcd}\langle kl|\hat{v}|cd\rangle\, t_{ik}^{ac}t_{lj}^{db} \tag{6.24}$$

$$-\frac{1}{2}\hat{P}(ij)\sum_{klcd}\langle kl|\hat{v}|cd\rangle\, t_{ik}^{ab}t_{jl}^{cd} - \frac{1}{2}\hat{P}(ab)\sum_{klcd}\langle kl|\hat{v}|cd\rangle\, t_{kl}^{bd}t_{ij}^{ac} \tag{6.25}$$

Labeling each term for practical reasons

$$L_a = \frac{1}{2}\sum_{cd}\langle ab|\hat{v}|cd\rangle\, t_{ij}^{cd} \tag{6.26}$$

$$L_b = \frac{1}{2}\sum_{kl}\langle kl|\hat{v}|ij\rangle\, t_{kl}^{ab} \tag{6.27}$$

$$L_c = \hat{P}\,(ij|ab)\sum_{kc}\langle kb|\hat{v}|cj\rangle\, t_{ik}^{ac} \tag{6.28}$$

$$Q_a = \frac{1}{4}\sum_{klcd}\langle kl|\hat{v}|cd\rangle\, t_{ij}^{cd}t_{kl}^{ab} \tag{6.29}$$

$$Q_b = \frac{1}{2}\hat{P}\,(ij|ab)\sum_{klcd}\langle kl|\hat{v}|cd\rangle\, t_{ik}^{ac}t_{lj}^{db} \tag{6.30}$$

$$Q_c = -\frac{1}{2}\hat{P}(ij)\sum_{klcd}\langle kl|\hat{v}|cd\rangle\, t_{ik}^{ab}t_{jl}^{cd} \tag{6.31}$$

$$Q_d = -\frac{1}{2}\hat{P}(ab)\sum_{klcd}\langle kl|\hat{v}|cd\rangle\, t_{kl}^{bd}t_{ij}^{ac} \tag{6.32}$$

6.3 Intermediates

As Coupled Cluster computations are consume large amounts of computational power, researchers are spending much effort trying to reduce computational cost. One way of reducing the cost is by refactoring the amplitude equations such that we can perform an intermediate computation first and use the result to compute various diagrams later.

Rewriting the equation, (6.20) for CCD amplitudes (Source: Gustav Baardsen

/ Audun):

$$(\epsilon_i + \epsilon_j - \epsilon_a - \epsilon_b)t_{ij}^{ab} = \langle ab|\hat{v}|ij\rangle + \frac{1}{2}\sum_{cd}\langle ab|\hat{v}|cd\rangle\, t_{ij}^{cd} \tag{6.33}$$

$$+\frac{1}{2}\sum_{kl} t_{kl}^{ab}\left[\langle kl|\hat{v}|ij\rangle + \frac{1}{2}\sum_{cd}\langle kl|\hat{v}|cd\rangle\, t_{ij}^{cd}\right] \tag{6.34}$$

$$+\hat{P}\,(ij|ab)\sum_{kc} t_{ik}^{ac}\left[\langle kb|\hat{v}|cj\rangle + \frac{1}{2}\sum_{ld}\langle kl|\hat{v}|cd\rangle\, t_{lj}^{db}\right] \tag{6.35}$$

$$-\frac{1}{2}\hat{P}(ij)\sum_{k} t_{ik}^{ab}\left[\sum_{lcd}\langle kl|\hat{v}|cd\rangle\, t_{jl}^{cd}\right] \tag{6.36}$$

$$-\frac{1}{2}\hat{P}(ab)\sum_{c} t_{ij}^{ac}\left[\sum_{kld}\langle kl|\hat{v}|cd\rangle\, t_{kl}^{bd}\right] \tag{6.37}$$

We can now define, and precompute the following values

$$I_1 = \langle kl|\hat{v}|ij\rangle + \frac{1}{2}\sum_{cd}\langle kl|\hat{v}|cd\rangle\, t_{ij}^{cd} \tag{6.38}$$

$$I_2 = \langle kb|\hat{v}|cj\rangle + \frac{1}{2}\sum_{ld}\langle kl|\hat{v}|cd\rangle\, t_{lj}^{db} \tag{6.39}$$

$$I_3 = \sum_{lcd}\langle kl|\hat{v}|cd\rangle\, t_{jl}^{cd} \tag{6.40}$$

$$I_4 = \sum_{kld}\langle kl|\hat{v}|cd\rangle\, t_{kl}^{bd} \tag{6.41}$$

We can now redefine the CCD equation

$$(\epsilon_i + \epsilon_j - \epsilon_a - \epsilon_b)t_{ij}^{ab} = \langle ab|\hat{v}|ij\rangle + \frac{1}{2}\sum_{cd}\langle ab|\hat{v}|cd\rangle\, t_{ij}^{cd} + \frac{1}{2}\sum_{kl} t_{kl}^{ab} I_1 \tag{6.42}$$

$$+\hat{P}\,(ij|ab)\sum_{kc} t_{ik}^{ac} I_2 - \frac{1}{2}\hat{P}(ij)\sum_{k} t_{ik}^{ab} I_3 - \frac{1}{2}\hat{P}(ab)\sum_{c} t_{ij}^{ac} I_4 \tag{6.43}$$

Leading to a reduction of computational cost from $\mathcal{O}(h^4p^4)$ to $\mathcal{O}(h^4p^2)$

Chapter 7

The Pairing Model

The first system I look at is the pairing model. The pairing model has four energy levels with degeneracy two, one for positive and negative spins. I have used a system consisting of four electrons filling up the four lower-most states up to the Fermi level.

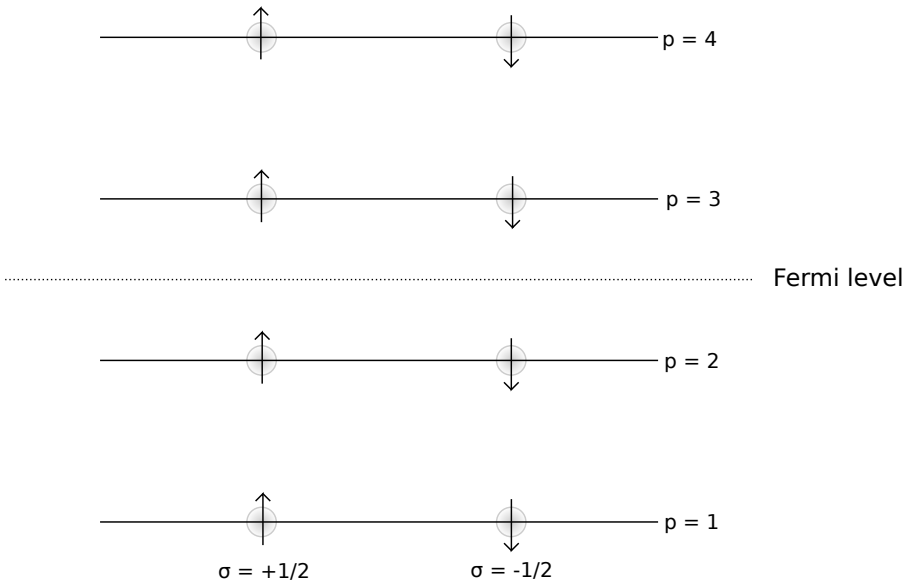

Figure 7.1: A figure depicting a 4 particles-4 holes state. The system consists of occupied particle states below the Fermi level and unoccupied hole states above Fermi level.

7.1 The Hamiltonian

We limit ourselves to a two-body interaction, writing the Hamiltonian as

$$\hat{H} = \sum_{\alpha\beta} \langle\alpha| \hat{h}_0 |\beta\rangle \hat{a}^\dagger_\alpha \hat{a}_\beta + \frac{1}{4} \sum_{\alpha\beta\gamma\delta} \langle\alpha\beta|\hat{v}_0|\gamma\delta\rangle \hat{a}^\dagger_\alpha \hat{a}^\dagger_\beta \hat{a}_\delta \hat{a}_\gamma \tag{7.1}$$

We use the complete basis $|\alpha\rangle$ and define the set as eigenvalues of the one-body operator, $\hat{h}_0$.

The system does require that the total spin is equal to 0. In addition we will not allow spin pairs to be broken, i.e. singly excitated states are not allowed.

$$|\Psi^a_i\rangle = 0 \tag{7.2}$$

We introduce the double creation and annihilation operator.

$$\hat{P}^\dagger_{pq} = \hat{a}^\dagger_{p\sigma} \hat{a}^\dagger_{p-\sigma} \tag{7.3}$$

$$\hat{P}_{pq} = a_{q\sigma} a_{q-\sigma} \tag{7.4}$$

We can rewrite the Hamiltonian as an unperterturbed part and a perturbation

$$\hat{H} = \hat{H}_0 + \hat{V} \tag{7.5}$$

$$\hat{H}_0 = \xi \sum_{p\sigma} (p-1) \hat{a}^\dagger_{p\sigma} \hat{a}_{p\sigma} \tag{7.6}$$

$$\hat{V} = -\frac{1}{2} g \sum_{pq} \hat{a}^\dagger_{p+} \hat{a}^\dagger_{p-} \hat{a}_{q-} \hat{a}_{q+} \tag{7.7}$$

The value of ξ determines the spacing between the energy levels, which I have set to 1. This will not impact the insight attained solving this system. p and q determines the energy level. σ is the spin, with value either $+\frac{1}{2}$ or $-\frac{1}{2}$. Both the unperturbed and perturbed Hamiltonian keeps total spin at 0

We can normal order the Hamiltonian by Wicks general theorem.

$$a^\dagger_p a_q = \left\{a^\dagger_p a_q\right\} + \delta_{pq\in i} \tag{7.8}$$

$$a^\dagger_p a^\dagger_q a_s a_r = \left\{a^\dagger_p a^\dagger_q a_s a_r\right\} + \left\{a^\dagger_p a_r\right\} \delta_{qs\in i} - \left\{a^\dagger_p a_s\right\} \delta_{qr\in i} \tag{7.9}$$

$$+ \left\{a^\dagger_q a_s\right\} \delta_{pr\in i} \; - \left\{a^\dagger_q a_r\right\} \delta_{ps\in i} + \delta_{pr\in i}\delta_{qs\in i} - \delta_{ps\in i}\delta_{qr\in i} \tag{7.10}$$

Which gives the Normal-ordered Hamiltonian

$$\hat{H} = \hat{H}_N + E_{ref} \tag{7.11}$$

$$\hat{H}_N = \hat{F}_N + \hat{W} \tag{7.12}$$

$$\hat{F}_N = \sum_{pq} h_{pq} \left\{ \hat{a}^\dagger_{p\sigma} \hat{a}_{p\sigma} \right\} - \sum_{pqi} \langle pi||qi\rangle \left\{ \hat{a}^\dagger_{p+} \hat{a}_{q-} \right\} \tag{7.13}$$

$$\hat{W} = -\frac{1}{2} \sum_{pqrs} \langle pq||rs\rangle \left\{ \hat{a}^\dagger_{p+} \hat{a}^\dagger_{p-} \hat{a}_{q-} \hat{a}_{q+} \right\} \tag{7.14}$$

$$E_{ref} = \sum_i h_{ii} + \frac{1}{2} \sum_{ij} \langle ij||ij\rangle \tag{7.15}$$

7.2 Configuration Interaction theory

This system is a good way to benchmark various methods as we can compute the exact solution using Full Configuration Interaction.

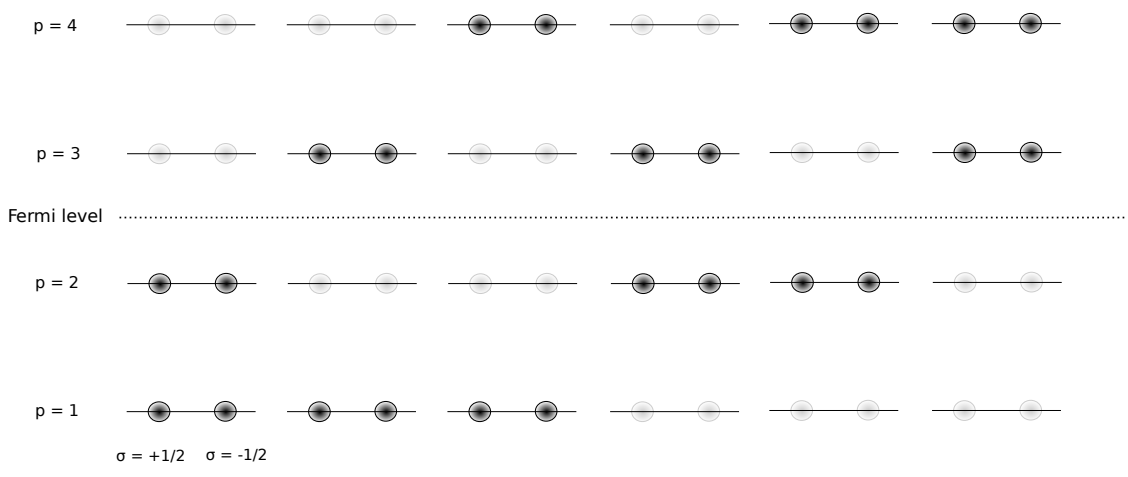

Figure 7.2: Configuration space for given pairing model showing all possible distributions of electrons

We need to diagonalize the Hamiltonian matrix looking at the linear combination of all different compinations of

$$\hat{\mathcal{H}} = \begin{pmatrix} & |\Phi_0\rangle & |\Phi_{12}^{56}\rangle & |\Phi_{12}^{78}\rangle & |\Phi_{34}^{56}\rangle & |\Phi_{34}^{78}\rangle & |\Phi_{1234}^{5678}\rangle \\ \langle\Phi_0| & & & & & & \\ \langle\Phi_{12}^{56}| & & & & & & \\ \langle\Phi_{12}^{78}| & & & & & & \\ \langle\Phi_{34}^{56}| & & & & & & \\ \langle\Phi_{34}^{78}| & & & & & & \\ \langle\Phi_{1234}^{5678}| & & & & & & \end{pmatrix} \tag{7.16}$$

Excluding the 4p-4h excitations one does not diagonalize the exact matrix, but rather the approximated matrix known from Configuration Interaction.

The diagonal elements are calculated using Wick's theorem. Looking first at the ground state calculation with the unperturbed Hamiltonian part

$$\left\langle \Phi_0 \middle| \hat{\mathbf{H}}_\mathbf{0} \middle| \Phi_0 \right\rangle \tag{7.17}$$

$$\langle |\, a_{2\downarrow} a_{2\uparrow} a_{1\downarrow} a_{1\uparrow} \sum_{p\sigma} \delta(p-1) a_{p\sigma}^\dagger a_{p\sigma} a_{1\uparrow}^\dagger a_{1\downarrow}^\dagger a_{2\uparrow}^\dagger a_{2\downarrow}^\dagger \,| \rangle \tag{7.18}$$

Which we see can contract in four different ways, resulting in

$$2\delta(1-1) + 2\delta(2-1) = 2\delta \tag{7.19}$$

And the perturbation part

$$\left\langle \Phi_0 \middle| \hat{\mathbf{V}} \middle| \Phi_0 \right\rangle \tag{7.20}$$

$$\langle |\, a_{2\downarrow} a_{2\uparrow} a_{1\downarrow} a_{1\uparrow} \left(-g/2 \sum_{pq} a_{p\uparrow}^\dagger a_{q\downarrow}^\dagger a_{q\downarrow} a_{p\uparrow} \right) a_{1\uparrow}^\dagger a_{1\downarrow}^\dagger a_{2\uparrow}^\dagger a_{2\downarrow}^\dagger \,| \rangle \tag{7.21}$$

As we can see, there are two ways this can contract, each contributing with the constant factor, $-g/2$ Resulting in the final Hamiltonian matrix

$$\hat{\mathcal{H}} = \begin{pmatrix} 2\delta - g & -g/2 & -g/2 & -g/2 & -g/2 & 0 \\ -g/2 & 4\delta - g & -g/2 & -g/2 & 0 & -g/2 \\ -g/2 & -g/2 & 6\delta - g & 0 & -g/2 & -g/2 \\ -g/2 & -g/2 & 0 & 6\delta - g & -g/2 & -g/2 \\ -g/2 & 0 & -g/2 & -g/2 & 8\delta - g & -g/2 \\ 0 & -g/2 & -g/2 & -g/2 & -g/2 & 10\delta - g \end{pmatrix} \tag{7.22}$$

7.3 Hartree-Fock calculations

When doing Hartree-Fock calculations on the pairing model, the goal is to minimize the Hamiltonian expectation value through a change in basis. The ground state energy is given by

$$\langle \Phi_0 | \hat{H} | \Phi_0 \rangle = E^{\mathrm{HF}} \tag{7.23}$$

This leads to the iterative equation

$$\sum_{\gamma} h^{\mathrm{HF}}_{\alpha\gamma} C_{a\gamma} = \epsilon_a C_{a\alpha} \tag{7.24}$$

where

$$h^{\mathrm{HF}}_{\alpha\gamma} = \langle \alpha | h | \gamma \rangle + \sum_{b=1}^{N} \sum_{\beta\delta} C^*_{b\beta} C_{b\delta} \langle \alpha\beta | v | \gamma\delta \rangle \tag{7.25}$$

For the first iteration, we must make a guess on the factors, $C^*_{b\beta}$ and $C_{b\delta}$. A natural starting point is to set

$$C_{b\beta} = \delta_{b\beta} \qquad C_{b\delta} = \delta_{b\delta} \tag{7.26}$$

This is the same as saying we use the original basis in the first iteration, as there is no overlap between the states

$$|\psi_a\rangle = \sum_{\lambda} \delta_{a\lambda} |\psi_\lambda\rangle \tag{7.27}$$

To evaluate the hatree-fock matrix elements, we look at the states below Fermi level

$$\{p, \sigma\} \in \{1\uparrow, 1\downarrow, 2\uparrow, 2\downarrow\} \tag{7.28}$$

The greek basis will therefore loop over these four states. The one-electron operator $\hat{H}_0$ is diagonal, so the matrix element

$$\langle \alpha | h | \gamma \rangle \tag{7.29}$$

Will also be diagonal. Because of the starting point for the basis coefficients, we see that the two-electron operator can be written as

$$V = \sum_{b=1}^{4} \langle \alpha b | v | \gamma b \rangle \tag{7.30}$$

Because the pairing model do not allow broken pairs, this matrix element will only be non-zero when $\alpha = \gamma$ and when $p_\alpha = p_b$, $\sigma_\alpha = \sigma_b$. The Hartree-Fock matrix will therefore be diagonal, meaning the original basis is a canonical Hartree-Fock basis. Hartree-Fock calculations on this basis will not provide any new results. The Hartree-Fock energy can be calculated

$$E^{\mathrm{HF}} = \langle \Phi_0 | \hat{H} | \Phi_0 \rangle = \langle \Phi_0 | \hat{H}_0 | \Phi_0 \rangle + \langle \Phi_0 | \hat{V} | \Phi_0 \rangle \tag{7.31}$$

$$= 2 - g \tag{7.32}$$

This energy will be referred to as the reference energy

7.4 Many-Body Perturbation Theory

When setting up the MBPT equations, it is useful to present them as diagrams. All the diagrams for the first, second and third order perturbation theory can be presented in figure ()

Because of special properties of the Pairing model, many of these diagrams can be removed by a visual examination. First, we have no broken pairs, meaning that a general two-body matrix element

$$\langle pq|v|rs\rangle \tag{7.33}$$

is only non-zero if *both* p and q are hole states or *both* are particle states. The same restriction applies to r and s. The second thing to notice, is that we have a canonical Hartree-Fock. That means only diagonal one-body matrix elements are non-zero. We will compute the correlation energy ΔE, using the Hamiltonian

$$\hat{H}_N = \hat{F}_N^d + \hat{F}_N^o + \hat{W} = \hat{F}_N^d + \hat{W} \tag{7.34}$$

where

$$f_{pq} = \epsilon_p \delta_{pq} \tag{7.35}$$

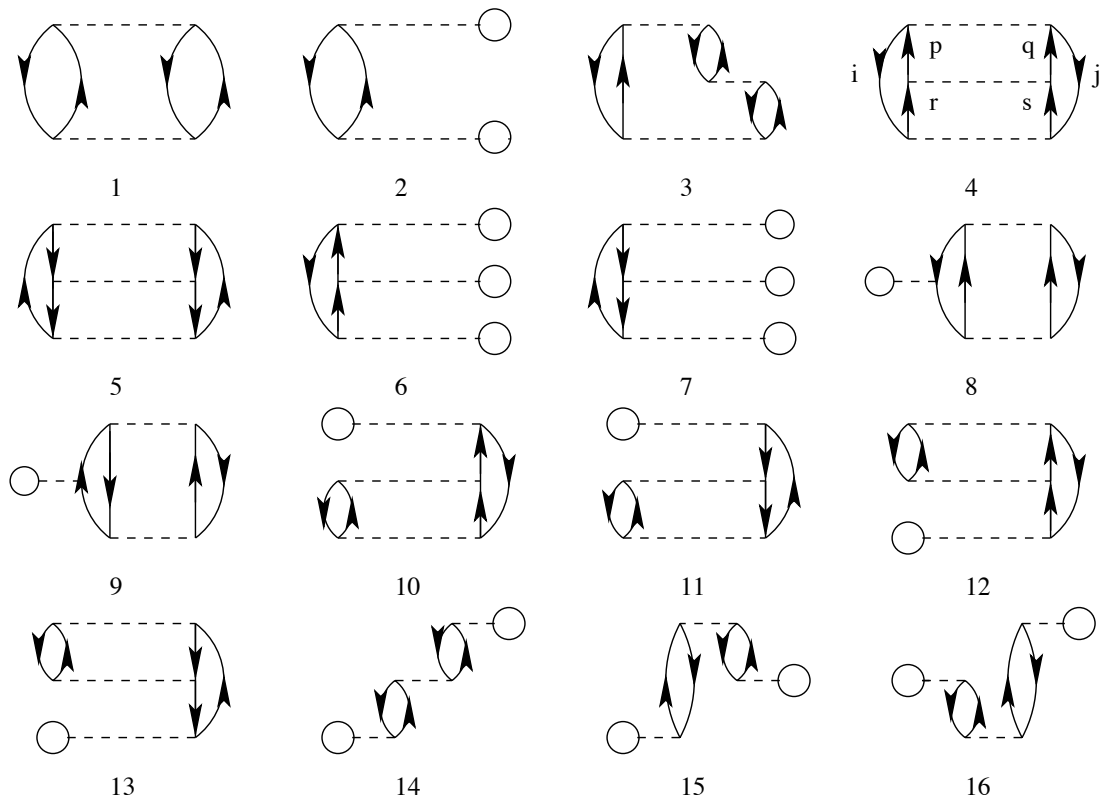

Figure 7.3: Diagrams for Many Body Perturbation theory to second and third order.

7.4.1 Interpreting diagrams

When reading the diagrams, and connecting them to the equations presented in the equations (5.41), there are a simple set of rules. We have the expression for the resolvent, $\hat{R}_0$ given as

$$\hat{R}_0 = \frac{\hat{Q}}{E_0^{(0)} - \hat{H}_0} = \sum_I \frac{|\Phi_I\rangle \langle \Phi_I|}{E_0^{(0)} - E_I^{(0)}} \tag{7.36}$$

Where we sum over all states apart from $|\Phi_0\rangle$. When this operator operates on any state $|J\rangle$ other than $|\Phi_0\rangle$, it will only produce [3]

$$\hat{R}_0 |J\rangle = |J\rangle \frac{1}{E_0^{(0)} - E_J^{(0)}} \tag{7.37}$$

Meaning that the resolvent will only introduce a denominator expressed in terms of zeroth-order energies. We will introduce a more practical notation for this

denominator

$$\epsilon_{ij..}^{ab..} = E_0^{(0)} - E_{\left|\Phi_{ij..}^{ab..}\right\rangle} = \epsilon_i + \epsilon_j + ... - \epsilon_a - \epsilon_b - ... \tag{7.38}$$

The operator $\hat{V}$, as shown in equations (5.41), will give rise to matrix elements. If we have a canonical Hartree-Fock basis, we can rewrite

$$\hat{V} = \hat{W} + \hat{F}^o = \hat{W} \tag{7.39}$$

And there will only be two-body matrix elements present and all diagrams with one-body interactions can be removed. In the noncanonical Hartree-Fock case, $\hat{F}^o$ will give non-zero results and must be present. The procedure for interpreting the diagram and write out the corresponding equations can be summed up in the following sequence of operations

7.4.2 Label all lines

First one should identify which lines represent hole states and which represent particle states, and label the lines with the corresponding letter, using $i, j, k, l, ...$ for hole states and $a, b, c, d, ...$ for particle states.

7.4.3 Identify the operators

A one-body vertex should be identified as the one body operator used for the system, where one set up the matrix element f_p^q by the labels as

$$f_p^q = \langle \text{line out} | \, \hat{f} \, | \text{line in} \rangle \tag{7.40}$$

The two-body vertices are identified as the two body operators, and when identified, one should set up the corresponding matrix elements following the interpretation rule

$$\langle pq||rs\rangle = \langle \text{left in, right in}||\text{left out, right out}\rangle \tag{7.41}$$

7.4.4 Identify the denominator

To identify the denominator produced by the resolvent, $\hat{R}_0$, one draws imaginary lines between the interactions and set up the ϵ for every state-line that was crossed

7.4.5 Including phase factor

The resulting diagram will get a phase factor depending on how many hole states and how many closed loops there are. The factor is given by

$$(-1)^{\text{Closed loops+Number of holes}} \tag{7.42}$$

7.4.6 Identify equivalent lines

Equivalent lines are pairs of lines that connect at the same vertices. They must also have be of the same kind, either both particle states or both hole states. They will introduce a factor given as

$$\left(\frac{1}{2}\right)^{\text{number of equivalent lines}} \tag{7.43}$$

7.4.7 Second Order Perturbation Theory

Starting with diagram 1, we see that this diagram is non-zero, because there is no one-body operator and no pairs are broken. We can set up the equation as

$$E_{\text{Diagram 1}} = (-1)^{2+2}\frac{1}{2^2}\sum_{\substack{ab\\ij}}\frac{\langle ij||ab\rangle\langle ab||ij\rangle}{\epsilon_{ij}^{ab}} \tag{7.44}$$

Diagram 2 can be written out as

$$E_{\text{Diagram 2}} = \sum_{ia}\frac{\langle i|\, f\,|a\rangle\langle a|\,\hat{f}\,|i\rangle}{\epsilon_i^a} = 0 \tag{7.45}$$

This, however, will be zero. This is because we are operating with a canonical Hartree-Fock basis. By the definition of a non canonical Hartree Fock basis, $f_i^a = 0$, that basis would provide the same result. That means, only diagram 1 will provide a non-zero result for second order perturbation theory.

7.4.8 Third Order Perturbation Theory

Looking at the third order diagrams, shown in figure () , numbering from 3 to 15. Third order diagrams have three interaction parts. One at the top and one at the bottom of the diagram along with an intermediate interaction part in the

middle. As we did for diagram 2, we can exclude all diagrams with a one-body operator, leaving only diagrams 3, 4 and 5.

$$E_{\text{diagram 3}} = \sum_{\substack{abc \\ ijk}} \frac{\langle ij||ab\rangle \langle bk||jc\rangle \langle ac||ij\rangle}{\epsilon_{ij}^{ac}\epsilon_{ij}^{ab}} = 0 \tag{7.46}$$

However, here we see a problem. We have an interaction term $\langle bk||jc\rangle$, which is a broken pair. The Pairing model do not allow such states, and this must be zero. This is not a problem for the diagrams 4 and 5.

$$E_{\text{diagram 4}} = \frac{1}{2^3} \sum_{\substack{abcd \\ ij}} \frac{\langle cd||ij\rangle \langle ab||cd\rangle \langle ij||ab\rangle}{\epsilon_{ij}^{cd}\epsilon_{ij}^{ab}} \tag{7.47}$$

$$E_{\text{diagram 4}} = \frac{1}{2^3} \sum_{\substack{ab \\ ijkl}} \frac{\langle ab||kl\rangle \langle kl||ij\rangle \langle ij||ab\rangle}{\epsilon_{kl}^{ab}\epsilon_{ij}^{ab}} \tag{7.48}$$

So when doing perturbation theory to third degree with a canonical Hartree-Fock basis as for the Pairing model, one only need to calculate the diagrams 1, 4 and 5.

7.4.9 Fourth Order Perturbation Theory

When calculating the correlation energy with the fourth order energy, the second and third order are included as well. The amount of diagrams increase dramatically when adding the fourth order, but as we only work with a canonical Hartree-Fock basis, the amount is somewhat limited [3]. We group the diagrams by the excitations they produce, i.e. how many pairs of external lines.

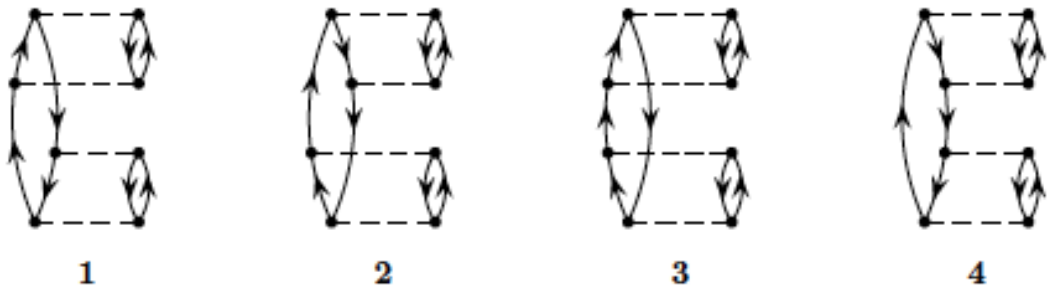

Figure 7.4: Goldstone diagrams for fourth order reileigh schrodinger perturbation theory with 1p1h excitations

The first set of diagrams in figure (7.4) show diagrams giving rise to 1 particle

and 1 hole excitations. All these diagrams have an intermediate step with a 1p-1h part. The Pairing model do not allow broken pairs, meaning that intermediate steps with 1p-1h or 3p-3h interaction parts must be zero. Therefore none of these diagrams are included in the calculations.

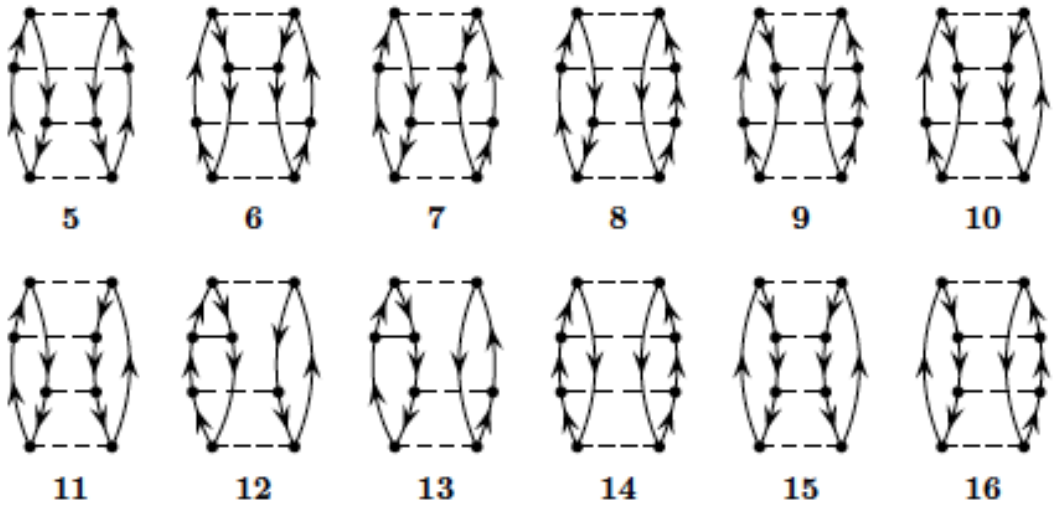

Figure 7.5: Goldstone diagrams for fourth order reileigh schrodinger perturbation theory with 2p2h excitations

The set of diagrams shown in figure (7.5), give rise to a 2 particle and 2 hole excitation. For all these diagrams, there are only 2p-2h interaction parts for all intermediate steps. However, many of these diagrams give rise to a broken pair interaction of the form

$$\langle ai||pq\rangle \tag{7.49}$$

Only the diagrams 5,6,14 and 15 have no broken pair interactions. They are calculated as

$$E_{\text{diagram 5}} = \frac{1}{2^4}\sum_{\substack{abcd\\ijkl}} \frac{\langle cd||kl\rangle\,\langle kl||ij\rangle\,\langle ab||cd\rangle\,\langle ij||ab\rangle}{\epsilon^{cd}_{kl}\epsilon^{cd}_{ij}\epsilon^{ab}_{ij}} \tag{7.50}$$

And diagram 6

$$E_{\text{diagram 6}} = \frac{1}{2^4}\sum_{\substack{abcd\\ijkl}} \frac{\langle cd||kl\rangle\,\langle kl||ij\rangle\,\langle ab||cd\rangle\,\langle ij||ab\rangle}{\epsilon^{ab}_{kl}\epsilon^{cd}_{kl}\epsilon^{ab}_{ij}} \tag{7.51}$$

For diagram 14, we get

$$E_{\text{diagram 14}} = \frac{1}{2^4} \sum_{\substack{abcdef \\ ij}} \frac{\langle ij||ab\rangle \langle ab||cd\rangle \langle cd||ef\rangle \langle ef||ij\rangle}{\epsilon_{ij}^{ab}\epsilon_{ij}^{cd}\epsilon_{ij}^{ef}} \tag{7.52}$$

And for diagram 15

$$E_{\text{diagram 15}} = \frac{1}{2^4} \sum_{\substack{ab \\ ijklmn}} \frac{\langle ij||ab\rangle \langle kl||ij\rangle \langle mn||kl\rangle \langle ab||mn\rangle}{\epsilon_{ij}^{ab}\epsilon_{kl}^{ab}\epsilon_{mn}^{ab}} \tag{7.53}$$

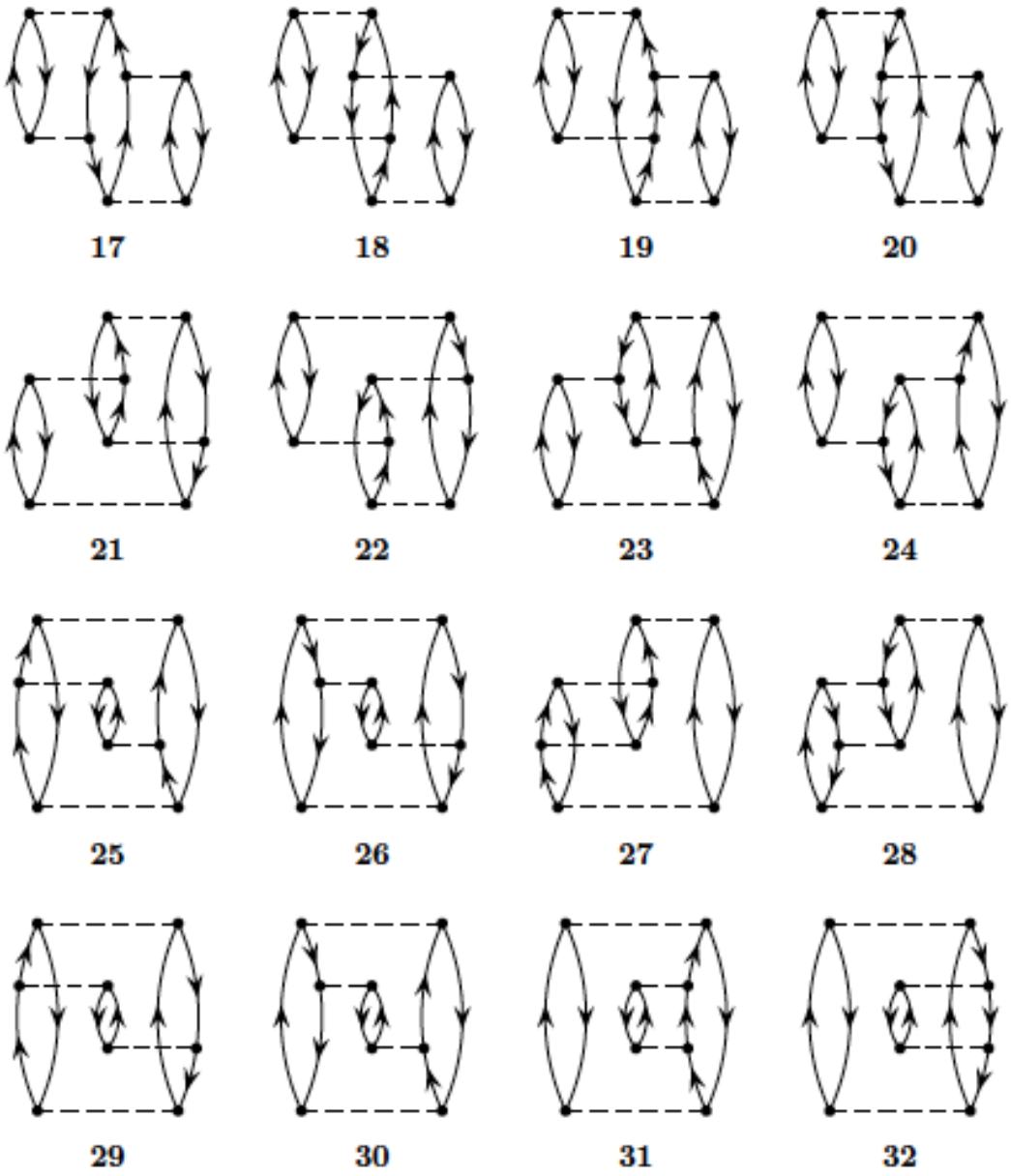

Figure 7.6: Goldstone diagrams for fourth order reileigh schrodinger perturbation theory with 3p3h excitations

The diagrams depicted in figure (7.6), show the fourth order diagrams giving rise to 3 particles and 3 holes excitations. We notice that all these diagrams include one intermediate step with a 3p-3h excitation. Therefore we can exclude all these diagrams from the calculations.

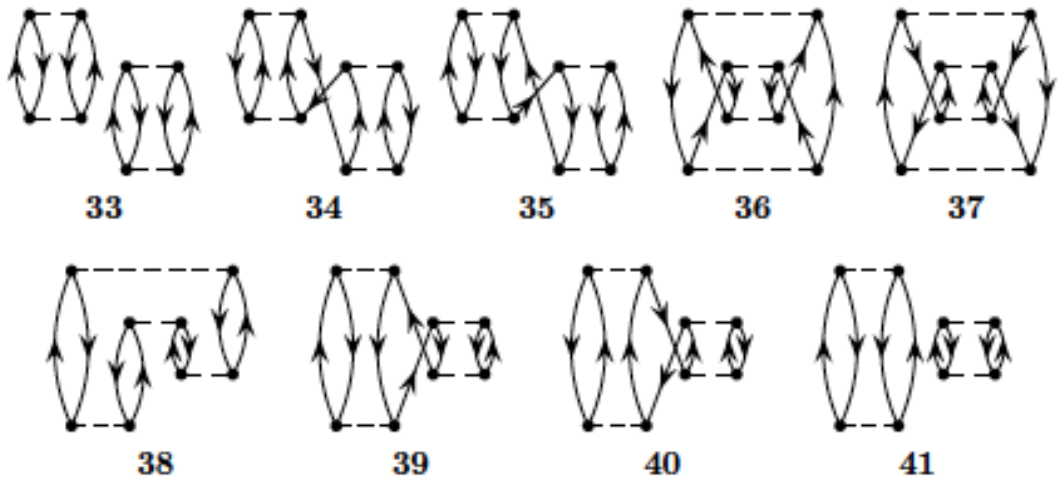

Figure 7.7: Goldstone diagrams for fourth order Reileigh Schrodinger perturbation theory with 4p4h excitations

The last set of diagrams, depicted in figure (7.7), show the fourth order diagrams that include a 4 particle and 4 hole part. Invoking the Linked diagram theorem, we can immediatly exclude diagram 33 and diagram 41. Diagram 34 to 40 do will be non-zero, and must be calculated. For diagram 34, we get

$$E_{\text{diagram 34}} = (-1)^{(3+4)} \frac{1}{2^2} \sum_{\substack{abcd \\ ijkl}} \frac{\langle ij||ab\rangle \langle kl||cd\rangle \langle ab||ik\rangle \langle cd||jl\rangle}{\epsilon_{ij}^{ab} \epsilon_{ijkl}^{abcd} \epsilon_{jl}^{cd}} \tag{7.54}$$

We notice that there are 3 closed loops and 4 hole states, giving rise to the negative phase factor. We also notice that we have two pairs of equivalent lines, arising from the particle states, introducing a factor $\frac{1}{4}$. One can also notice the fourth order denominator term ϵ_{ijkl}^{abcd}, arising from the 4p-4h intermediate excitation part. The last diagrams are calculated following the same principles, giving

$$E_{\text{diagram 35}} = (-1)^{(3+4)} \frac{1}{2^2} \sum_{\substack{abcd \\ ijkl}} \frac{\langle ij||ab\rangle \langle kl||cd\rangle \langle ac||ij\rangle \langle bd||kl\rangle}{\epsilon_{ij}^{ab} \epsilon_{ijkl}^{abcd} \epsilon_{kl}^{bd}} \tag{7.55}$$

And diagram 36. Please notice that there are a mistake in the drawing of the diagram 36. The right-most particle state is supposed to be a hole state, giving the correct equation

$$E_{\text{diagram 36}} = \frac{1}{2^4} \sum_{\substack{abcd \\ ijkl}} \frac{\langle ij||ab\rangle \langle kl||cd\rangle \langle ab||kl\rangle \langle cd||ij\rangle}{\epsilon_{ij}^{ab} \epsilon_{ijkl}^{abcd} \epsilon_{ij}^{cd}} \tag{7.56}$$

Diagram 37 is also depicted with the right-most state wrong. It is supposed to be a particle state, giving

$$E_{\text{diagram 37}} = \frac{1}{2^4} \sum_{\substack{abcd \\ ijkl}} \frac{\langle ij||ab\rangle \langle kl||cd\rangle \langle cd||ij\rangle \langle ab||kl\rangle}{\epsilon_{ij}^{ab} \epsilon_{ijkl}^{abcd} \epsilon_{kl}^{ab}} \tag{7.57}$$

and for diagram 38, we notice that there are no equal state pairs

$$E_{\text{diagram 38}} = \sum_{\substack{abcd \\ ijkl}} \frac{\langle ij||ab\rangle \langle kl||cd\rangle \langle db||lj\rangle \langle ac||ik\rangle}{\epsilon_{ij}^{ab} \epsilon_{ijkl}^{abcd} \epsilon_{ik}^{ac}} \tag{7.58}$$

Diagram 39 gives

$$E_{\text{diagram 39}} = (-1)^{(3+4)} \frac{1}{2^2} \sum_{\substack{abcd \\ ijkl}} \frac{\langle ij||ab\rangle \langle kl||cd\rangle \langle bd||kl\rangle \langle ac||ij\rangle}{\epsilon_{ij}^{ab} \epsilon_{ijkl}^{abcd} \epsilon_{ij}^{ac}} \tag{7.59}$$

And finally, diagram 40 gives the equation

$$E_{\text{diagram 40}} = (-1)^{(3+4)} \frac{1}{2^2} \sum_{\substack{abcd \\ ijkl}} \frac{\langle ij||ab\rangle \langle kl||cd\rangle \langle cd||jl\rangle \langle ab||ik\rangle}{\epsilon_{ij}^{ab} \epsilon_{ijkl}^{abcd} \epsilon_{ik}^{ab}} \tag{7.60}$$

7.5 Spin Summations

We have up until now, not taken into account the effect of spin in the matrix elements. Because of spin orthogonality, terms may vanish from certain two-electron matrix elements. Listed here, are all the different ways spins can be organized, along with the resulting integration. Representing the spin up orbital with a bar, we get [3]

$$\langle pq||rs\rangle = \langle pq|\hat{v}|rs\rangle - \langle pq|\hat{v}|sr\rangle \tag{7.61}$$
$$\langle p\bar{q}||r\bar{s}\rangle = \langle pq|\hat{v}|rs\rangle \tag{7.62}$$
$$\langle p\bar{q}||\bar{r}s\rangle = -\langle pq|\hat{v}|sr\rangle \tag{7.63}$$
$$\langle \bar{p}q||\bar{r}s\rangle = \langle pq|\hat{v}|rs\rangle \tag{7.64}$$
$$\langle \bar{p}q||r\bar{s}\rangle = -\langle pq|\hat{v}|sr\rangle \tag{7.65}$$
$$\langle \bar{p}\bar{q}||\bar{r}\bar{s}\rangle = \langle pq|\hat{v}|rs\rangle - \langle pq|\hat{v}|sr\rangle \tag{7.66}$$

Because of the restrictions on the pairing model, the first and last equation will also be zero, because the states are not allowed to exist. Matrix elements, where there is an unequal amount of equal spin orbitals will all give zero as result as

well

$$\langle \bar{p}q||rs\rangle = \langle p\bar{q}||rs\rangle = \langle pq||\bar{r}s\rangle = \langle pq||r\bar{s}\rangle = 0 \tag{7.67}$$

$$\langle \bar{p}\bar{q}||rs\rangle = \langle pq||\bar{r}\bar{s}\rangle = 0 \tag{7.68}$$

$$\langle \bar{p}\bar{q}||\bar{r}s\rangle = \langle \bar{p}\bar{q}||r\bar{s}\rangle = \langle \bar{p}q||\bar{r}\bar{s}\rangle = \langle p\bar{q}||\bar{r}\bar{s}\rangle = 0 \tag{7.69}$$

Chapter 8

Infinite Matter

A study of infinite matter is the most comprehensible way of studying nuclear material. This thesis will study the infinite electron gas before the final study of nuclear material. This is done because of pedagogical reasons and because the electron gas has closed form solutions that provide important benchmarking for the code.

8.1 The Infinate Electron Gas

The infinite electron gas gives a good approximation to valence electrons in metal. The gas consist only of interacting electrons with a uniform background of charged ions. The whole system is charge neutral. We assume a finite cubic box as done in [13] and [14]. The box has a length L and volume $\Omega = L^3$, with N_e as the number of electrons with a charge density $\rho = N_e/\Omega$.

8.1.1 The Hamiltonian

The electrons interact with the sentral symmetric Colomb potential, $\hat{V}(\mathbf{r}_1, \mathbf{r}_2)$ depending only on the distance $|\mathbf{r}_1 - \mathbf{r}_2|$. The Hamiltonian for infinite electron gas is [1]

$$\hat{H} = \hat{H}_1 + \hat{H}_2 = \hat{H}_{\text{kin}} + \hat{H}_{\text{interaction}} \tag{8.1}$$

The interaction term will be dependent on both the electron-electron interaction, the electron-background interaction and the background-background interaction

$$\hat{H} = \hat{H}_{\text{kin}} + \hat{H}_{\text{ee}} + \hat{H}_{\text{eb}} + \hat{H}_{\text{bb}} \tag{8.2}$$

And the kinetic energy, $\hat{H}_{\text{kin}}$ is given as

$$\hat{H}_{\text{kin}} = \sum_{p} \frac{\hbar^2 k^2}{2m} a^{\dagger}_{k\sigma} a_{k\sigma} \tag{8.3}$$

The background-interaction terms will vanish as explained by Fraser et al [16] both for three- and two-dimensional electron gas. When we sum over all particles, we can write the electron-electron interaction term as an Ewald summation term, because it is not possible to use a $1/r$ term for infinite systems [15] [21]. We can write this term as

$$\hat{H}_{ee} = \sum_{i<j}^{N} v_E(\mathbf{r}_i - \mathbf{r}_j) + \frac{1}{2} N e^2 v_0 \tag{8.4}$$

Where $v_E(\mathbf{r})$ is an effective two-body interaction. v_0 is the self-interaction term, defined as

$$v_0 = \lim_{\mathbf{r}\to\infty} \left\{ v_E(\mathbf{r}) - \frac{1}{r} \right\} \tag{8.5}$$

The Ewald summation will account for interactions between all electrons in the finite size system as well as all the image electrons that will arize from self-interaction because of periodic boundaries. We define it as

$$v_E(\mathbf{r}) = \sum_{k\neq 0} \frac{4\pi}{L^3 k^2} e^{i\mathbf{k}\cdot\mathbf{r}} e^{-\eta^2 k^2/4} \tag{8.6}$$

$$+ \sum_{\mathbf{R}} \frac{1}{|\mathbf{r}-\mathbf{R}|} \text{erfc}\left(\frac{|\mathbf{r}-\mathbf{R}|}{\eta} \right) - \frac{\pi\eta^2}{L^3} \tag{8.7}$$

L is the size of the box, $\mathbf{k}$ is the momentum vector, while $\mathbf{r}$ represent the position vectors for all electrons. The translational vector$\mathbf{R}$ is used to obtain all image cells in the entire real space [21]

$$\mathbf{R} = L(n_x \mathbf{u}_x + n_y \mathbf{u}_y + n_z \mathbf{u}_z) \tag{8.8}$$

We have used the error functions

$$\text{erf}(x) = \frac{2}{\sqrt{\pi}} \int_0^x e^{-t^2} \text{dt} \tag{8.9}$$

$$\text{erfc}(x) = 1 - \text{erf}(x) = \frac{2}{\sqrt{\pi}} \int_x^{\infty} e^{-t^2} \text{dt} \tag{8.10}$$

We use this relation because an interaction on the form $1/|r|$ is not convergent for an infinite number of particle [2]. Ewald found that one can rewrite the interaction in terms of these error functions [17]

$$\frac{1}{r} = \frac{\text{erf}(\frac{1}{2}\sqrt{\eta}r)}{r} + \frac{\text{erfc}(\frac{1}{2}\sqrt{\eta}r)}{r} \tag{8.11}$$

One can calculate the two-dimensional Ewald term as well [1], resulting in

$$v_E^{\eta=0,z=0} = \sum_{\mathbf{k}\neq 0} \frac{2\pi}{L^2 k} e^{i\mathbf{k}\cdot\mathbf{r}_{xy}} \tag{8.12}$$

8.1.2 The Reference Energy

The reference energy for electron gas can be written as [1]

$$E_{\text{ref}} = \sum_i \langle i|h_0|i\rangle + \frac{1}{2}\sum_{ij} \langle ij||ij\rangle + \frac{1}{2}Av_0 \tag{8.13}$$

A is the number of electrons, and the term Av_0 is the so-called Madelung constant. It is how we incorporates the self-interaction term into the system. This factor will be larger for smaller system and vanish as we approach the thermodynamic limit.

8.1.3 The Fock Matrix Elements

The Fock Matrix Elements will be given as

$$\langle p|f|q\rangle = \frac{k_p^2}{2m}\delta_{\mathbf{k}_p\mathbf{k}_q}\delta_{m_{sp}m_{sq}} + \sum_i \langle pi||qi\rangle \tag{8.14}$$

We notice that the Fock Matrix elements can be written as a diagonal part plus the $\hat{U}$ operator. As we can see from (3.93) and (3.95), this means the perturbation can be written solely by the two-body interaction

$$\hat{V} = \frac{1}{4}\sum_{pqrs} \langle pq||rs\rangle\, \hat{p}^\dagger\hat{q}^\dagger\hat{s}\hat{r} \tag{8.15}$$

8.1.4 Anti-Symmetric Matrix Elements

We now need to define the matrix elements for the two- and three-dimensional electron gas to calculate the perturbation

$$\left\langle \mathbf{k}_p m_{s_p} \mathbf{k}_q m_{s_q} || \mathbf{k}_r m_{s_r} \mathbf{k}_s m_{s_s} \right\rangle \tag{8.16}$$

$$= \frac{4\pi e^2}{L^3} \delta_{\mathbf{k}_p+\mathbf{k}_q,\mathbf{k}_r+\mathbf{k}_s} \left\{ \delta_{m_{s_p},m_{s_r}} \delta_{m_{s_q},m_{s_s}} (1-\delta_{\mathbf{k}_p,\mathbf{k}_r}) \frac{1}{|\mathbf{k}_r-\mathbf{k}_p|^2} \right. \tag{8.17}$$

$$\left. - \delta_{m_{s_p},m_{s_s}} \delta_{m_{s_q},m_{s_r}} (1-\delta_{\mathbf{k}_p,\mathbf{k}_s}) \frac{1}{|\mathbf{k}_s-\mathbf{k}_p|^2} \right\} \tag{8.18}$$

The two-dimensial case is almost identical

$$\left\langle \mathbf{k}_p m_{s_p} \mathbf{k}_q m_{s_q} || \mathbf{k}_r m_{s_r} \mathbf{k}_s m_{s_s} \right\rangle \tag{8.19}$$

$$= \frac{2\pi e^2}{L^2} \delta_{\mathbf{k}_p+\mathbf{k}_q,\mathbf{k}_r+\mathbf{k}_s} \left\{ \delta_{m_{s_p},m_{s_r}} \delta_{m_{s_q},m_{s_s}} (1-\delta_{\mathbf{k}_p,\mathbf{k}_r}) \frac{1}{|\mathbf{k}_r-\mathbf{k}_p|} \right. \tag{8.20}$$

$$\left. - \delta_{m_{s_p},m_{s_s}} \delta_{m_{s_q},m_{s_r}} (1-\delta_{\mathbf{k}_p,\mathbf{k}_s}) \frac{1}{|\mathbf{k}_s-\mathbf{k}_p|} \right\} \tag{8.21}$$

8.1.5 The Plane Wave Basis

When set up with periodic boundary conditions, the Homogenous electron gas can be set up with free particle normalized wave functions

$$\psi_{\mathbf{k}\sigma}(\mathbf{r}) = \frac{1}{\sqrt{\Omega}} e^{i\mathbf{k}\mathbf{r}} \xi_\sigma \tag{8.22}$$

Where $\mathbf{k}$ is the wave number and ξ_σ is a spin function.

$$\xi_{+\frac{1}{2}} = \begin{pmatrix} 1 \\ 0 \end{pmatrix} \quad \xi_{-\frac{1}{2}} = \begin{pmatrix} 0 \\ 1 \end{pmatrix} \tag{8.23}$$

Because of periodic boundary conditions, we acquire the following wave numbers

$$k_i = \frac{2\pi n_i}{L} \quad i = x, y, z \quad n_i = 0, \pm 1, \pm 2, ... \tag{8.24}$$

and the associated single-particle energies for two dimensions

$$\epsilon_{n_x,n_y} = \frac{\hbar^2}{2m} \left(\frac{2\pi}{L} \right)^2 (n_x^2 + n_y^2) \tag{8.25}$$

And for three dimensions

$$\epsilon_{n_x,n_y,n_z} = \frac{\hbar^2}{2m}\left(\frac{2\pi}{L}\right)^2 (n_x^2 + n_y^2 + n_z^2) \tag{8.26}$$

By the nature of the single particle energies, the energy levels will be determined by the value of $n_x^2 + n_y^2 + n_z^2$. There are different combinations of n_x, n_y and n_z that set up each energy level. The cumulative number of particles needed to completely fill these energy states will be named *magic numbers* and are listed in table (8.1).

$n_x^2+n_y^2+n_z^2$	n_x	n_y	n_z	$N_{\uparrow\uparrow}$	$N_{\uparrow\downarrow}$	$N_{\uparrow\downarrow}\hat{\tau}$
0	0	0	0	1	2	4
1	1	0	0			
	-1	0	0			
	0	1	0			
	0	-1	0			
	0	0	1			
	0	0	-1	7	14	28
2	1	1	0			
	1	-1	0			
	1	0	1			
	1	0	-1			
	-1	1	0			
	-1	-1	0			
	-1	0	1			
	-1	0	-1			
	0	1	1			
	0	1	-1			
	0	-1	1			
	0	-1	-1	19	38	76
3	1	1	1			
	1	1	-1			
	1	-1	1			
	1	-1	-1			
	-1	1	1			
	-1	1	-1			
	-1	-1	1			
	-1	-1	-1	27	54	108
4	2	0	0			
	-2	0	0			
	0	2	0			
	0	-2	0			
	0	0	2			
	0	0	-2	33	66	132
5				57	114	228
6				81	162	324
7				81	162	324
8				93	186	372

Table 8.1: All magic numbers for three dimensional infinite matter. The table demonstrates how states will fill up energy levels. n_x, n_y and n_z represent momentum quantum numbers, $n_x^2+n_y^2+n_z^2$ represent energy level. $N_{\uparrow\uparrow}$ shows magic number without spin degeneracy, $N_{\uparrow\downarrow}$ adds two possible spins, and $N_{\uparrow\downarrow}\hat{\tau}$ also adds isospin degeneracy.

8.2 Infinite Nuclear Matter

Central to my thesis, is the study of infinite nuclear matter. I look at baryonic matter similar to the dense baryonic matter found in neutron stars. I limit the study to temperatures far below Fermi level. The matter is mostly made up of an equilibrium of baryons and leptons. In neutron star matter, we assume the equilibrium consist of protons, neutrons, electrons and muons with densities larger than 0.1fm$^-$3. The equilibrium conditions are specified by weak interactions

$$b_1 \to b_2 + l + \bar{\nu}_l \qquad b_2 + l \to b_1 + \nu_l \tag{8.27}$$

Where b represent either neutron or proton and $l$is either an electron or muon. ν_l is the corresponding neutrino.

Nuclear matter is a hypothetical system filling all of space at a uniform density. Symmetric nuclear matter (SNM) consist of equal numbers of protons of neutrons, while pure nuclear matter (PNM) consist only of neutrons. For finite-nucleus systems, the most difficult part is calculating the single particle wave function. For nuclear matter we can use plane wave basis and similar to electron gas, the difficult part is calculating the energy and the effective interaction between particles [11]. In my calculations, I have looked at pure nuclear matter.

8.3 Nuclear Interaction

Nuclear matter is composed of baryons, which interacts through the strong force.

8.3.1 The Minnesota Potential

The Minnesota Potential is given as

$$v(r) = (v_R + (1 + P_{12}^{\sigma})v_T/2 + (1 - P_{12}^{\sigma})v_S/2) \tag{8.28}$$

$$\cdot \left(\alpha + (2 - \alpha)P_{12}^{r}\right)/2 + (1 + m_{t,1})(1 + m_{t,2})\frac{e^2}{4r} \tag{8.29}$$

where r is given as $|\mathbf{r_1} - \mathbf{r_2}|$ and m_t is the isospin projection of particle 1 or 2. $m_t = \pm 1$. P_{12}^{σ} and P_{12}^{r} are exchange operators for spin and position, respectively [1]. Furthermore, we have used

$$v_R = v_{0R}e^{-k_R r^2}, \quad v_T = -v_{0T}e^{-k_T r^2}, \quad v_S = -v_{0S}e^{-k_s r^2} \tag{8.30}$$

Where the constants v_{0R}, v_{0T}, v_{0S}, k_R, k_T and k_S are given by [12]

1. $v_{0R} = 200\text{MeV}$, $k_R = 0.1487\text{fm}^{-2}$
2. $v_{0T} = 178\text{MeV}$, $k_T = 0.649\text{fm}^{-2}$

3. $v_{0S} = 91.85\text{MeV}$, $k_S = 0.465\text{fm}^{-2}$

Written by second quantisation, we want to calculate the two-body interaction

$$\langle k_p k_q|v|k_r k_s\rangle = \frac{V_0}{L^3}\left(\frac{\pi}{\alpha}\right)^{3/2} e^{-q^2/4\alpha}\delta_{\mathbf{k}_p+\mathbf{k}_q,\mathbf{k}_r+\mathbf{k}_s} \tag{8.31}$$

Where q is the relative momentum transfer

$$\mathbf{q} = \mathbf{p} - \mathbf{p}' \tag{8.32}$$

$$\mathbf{p} = \frac{1}{2}(\mathbf{k}_p - \mathbf{k}_q) \quad \mathbf{p}' = \frac{1}{2}(\mathbf{k}_r - \mathbf{k}_s) \tag{8.33}$$

We can now set up the two-body Matrix-elements for the Minnesota Potential

$$\langle \mathbf{k}_p\mathbf{k}_q|v|\mathbf{k}_r\mathbf{k}_s\rangle = \langle \mathbf{k}_p\mathbf{k}_q|\frac{1}{2}\left(V_R + \frac{1}{2}V_T + \frac{1}{2}V_S\right)|\mathbf{k}_r\mathbf{k}_s\rangle \tag{8.34}$$

$$+ \langle \mathbf{k}_p\mathbf{k}_q|\frac{1}{4}(V_T - V_S)P_{12}^{\sigma}|\mathbf{k}_r\mathbf{k}_s\rangle \tag{8.35}$$

$$- \langle \mathbf{k}_p\mathbf{k}_q|\frac{1}{2}\left(V_R + \frac{1}{2}V_T + \frac{1}{2}V_S\right)P_{12}^{\sigma}P_{12}^{\tau}|\mathbf{k}_r\mathbf{k}_s\rangle \tag{8.36}$$

$$- \langle \mathbf{k}_p\mathbf{k}_q|\frac{1}{4}(V_T - V_S)P_{12}^{\tau}|\mathbf{k}_r\mathbf{k}_s\rangle \tag{8.37}$$

Matrix elements for the spin and isospin exchange operators are

$$\langle \sigma_p\sigma_q|P_{12}^{\sigma}|\sigma_r\sigma_s\rangle = \delta_{\sigma_p,\sigma_s}\delta_{\sigma_q,\sigma_r} \tag{8.38}$$

One can see that these matrix elements come at a far greater computational cost than for electron-electron interaction in the electron gas. Therefore it is necessary to compute and store all elements instead of computing them "on the fly". Source: Lecture 1-2 infinite matter.

Chapter 9

Implementation of CCD

In this thesis I have created three different solvers for Coupled Cluster Doubles equations.

1. A naive brute force implementation of the equations summing over all variables.

2. A naive brute force implementation of intermediate equations summing over all variables.

3. Rewriting summations as matrix-matrix multiplications and exploiting various symmetry arguments one can set up a block implementation.

There is a significant performance leap between each method, but I have included the first two solvers for both educational and benchmarking purposes. The Pairing model with 4 particles and 4 holes is a small system that one can easily solve using the naive approach. After producing expected results with the naive solver, I have compared the more complicated solvers to the naive solver for all systems.

9.1 Implementing the CCD equations

The basic steps of all implemented CCD algorithms can be explained through these steps

1. Initialize amplitudes $t^{(0)} = 0$and $\Delta E^{(0)}_{CCD} = 0$

2. Update the amplitudes and calculate $\Delta E^{(1)}_{CCD}$

3. If $|\Delta E^{(1)}_{CCD} - \Delta E^{(0)}_{CCD}| \geq \epsilon$, update amplitudes and compute ΔE^{2}_{CCD}

4. Repeat until $|\Delta E^{(n+1)}_{CCD} - \Delta E^{(n)}_{CCD}| \leq \epsilon$

The difference between the three solvers I have implemented is the way I update amplitudes. The naive brute force solver loops over all indices when computing. An example of diagram L_a is shown below

```
for i in 0, ..., Nholes:
  for j in 0, ..., Nholes:
    for a in Nholes, ..., Nparticles:
      for b in Nholes, ..., Nparticles:
        for c in Nholes, ..., Nparticles:
          for d in Nholes, ..., Nparticles:
            tnew(a,b,i,j) = 0.5  v(a,b,c,d)  told(c,d,i,j)
```

A significant cost reduction can be obtained by factorizing the diagrams as shown in equation (6.43). By calculating the four intermediate diagrams, I_1, I_2, I_3 and I_4 beforehand and storing the results reduce the cost of calculation from $\mathcal{O}(h^4p^4)$ to $\mathcal{O}(h^4p^2)$. The second solver applies this method.

9.2 Matrix Representation of Contractions

Diagrams can be viewed as contractions of tensors of varying degree. An example is the matrix-matrix multiplication product

$$(MN)^{\alpha}_{\gamma} = \sum_{\beta} M^{\alpha}_{\beta} N^{\beta}_{\gamma} \tag{9.1}$$

As our goal is to rewrite the Coupled Cluster equations as matrix-matrix products. We will need to map tensors of rank ≥ 2 onto matrices. One mapping that provides systematic and unique matrix elements can be

$$\langle pq|\hat{v}|rs\rangle = V_{\alpha(p,q),\beta(r,s)} \tag{9.2}$$

Where

$$\alpha(p,q) = p + qN_p \quad \beta(r,s) = r + sN_r \tag{9.3}$$

We need to be careful when mapping tensors this way. Consider first the calculation of the perfectly aligned L_a term

$$L_a = \sum_{cd} \langle ab|\hat{v}|cd\rangle \, t^{cd}_{ij} \tag{9.4}$$

Mapping this equation using equation (9.3)

$$\langle ab|\hat{v}|cd\rangle = v^{cd}_{ab} \rightarrow V^{\alpha(a,b)}_{\beta(c,d)} \tag{9.5}$$

and

$$t_{ij}^{cd} \rightarrow T_{\delta(i,j)}^{\beta(c,d)} \tag{9.6}$$

As we are mapping to unique elements

$$\beta(c,d) = \beta(c,d) \tag{9.7}$$

We can now rewrite the equation

$$(L_a)_\delta^\alpha = \sum_\beta V_\beta^\alpha T_\delta^\beta \tag{9.8}$$

Implying by regarding equation (9.1) that we can rewrite the product as matrix-matrix multiplication

$$L_a = VT \tag{9.9}$$

9.2.1 Aligning elements

Unfortunately, not all product are perfectly aligned like L_a. Consider, for example, the term, L_c

$$L_c = -P\,(ij|ab) \sum_{kc} \langle kb|\hat{v}|cj\rangle\, t_{ik}^{ac} \tag{9.10}$$

Using the same mapping scheme

$$\langle kb|\hat{v}|cj\rangle = v_{cj}^{kb} \rightarrow V_{\beta(cj)}^{\alpha(kb)} \tag{9.11}$$

and

$$t_{ik}^{ac} \rightarrow T_{\delta(ik)}^{\gamma(ac)} \tag{9.12}$$

This matrix multiplication is misaligned, and if the number of particles is unequal to the number of holes, the matrices' size will uncompatible.

$$(L_c)_\delta^\alpha \neq -P\,(ij|ab) \sum_\beta V_{\beta(cj)}^{\alpha(kb)} T_{\delta(ik)}^{\gamma(ac)} \tag{9.13}$$

We need to find another mapping, such that

$$v_{cj}^{kb} \rightarrow \tilde{V}_{\beta(ck)}^{\alpha(bj)} \tag{9.14}$$

and

$$t_{ik}^{ac} \rightarrow \tilde{T}_{\delta(ia)}^{\gamma(ck)} \tag{9.15}$$

Now, the matrix multiplication is aligned

$$(\tilde{L}_c)_{\delta}^{\alpha} = -P\,(ij|ab) \sum_{\beta} \tilde{V}_{\beta(ck)}^{\alpha(bj)} \tilde{T}_{\delta(ia)}^{\gamma(ck)} \tag{9.16}$$

Note, however, that

$$L_c \neq \tilde{L}_c \tag{9.17}$$

We must "realign" $\tilde{L}_c$ to match the correct diagram

$$(\tilde{L}_c)_{\delta(i,a)}^{\alpha(b,j)} \rightarrow (L_c)_{\delta(i,k)}^{\alpha(k,b)} \tag{9.18}$$

Another example is the Qc term

$$Q_c = -\frac{1}{2}\hat{P}(ij) \sum_{klcd} \langle kl|v|cd\rangle\, t_{ik}^{ab} t_{jl}^{cd} \tag{9.19}$$

We can rewrite this as a matrix-matrix multiplication with the matrix elements given by

$$\langle kl|v|cd\rangle = v_{cd}^{kl} \rightarrow V_{\beta(kl)}^{\alpha(cd)} \tag{9.20}$$

$$t_{ik}^{ab} \rightarrow (T_1)_{\gamma(ik)}^{\delta(ab)} \tag{9.21}$$

$$t_{jl}^{cd} \rightarrow (T_2)_{\omega(jl)}^{\eta(cd)} \tag{9.22}$$

Because we sum over the coefficients $klcd$, we must make sure that they belong to the "inner" indexes. This can only be done by creating a hole, particle-particle-hole configuration. We must also change the order of multiplication

$$V_{\beta(kl)}^{\alpha(cd)} \rightarrow \tilde{V}_{\gamma(cdl)}^{\delta(k)} \tag{9.23}$$

$$(T_1)_{\gamma(ik)}^{\delta(ab)} \rightarrow \tilde{(T_1)}_{\delta(k)}^{\alpha(abi)} \tag{9.24}$$

$$(T_2)_{\omega(jl)}^{\eta(cd)} \rightarrow \tilde{(T_2)}_{\beta(j)}^{\gamma(cdl)} \tag{9.25}$$

This gives us

$$(\tilde{Q}_c)_{\beta(j)}^{\alpha(abi)} = -\frac{1}{2}\hat{P}(ij) \sum_{klcd} (\tilde{T}_1)_{\delta(k)}^{\alpha(abi)} \tilde{V}_{\gamma(cdl)}^{\delta(k)} (\tilde{T}_2)_{\beta(j)}^{\gamma(cdl)} \tag{9.26}$$

Which must be realigned back to the properly aligned Q_c before it can be added

to the amplitude equations.

$$(\tilde{Q}_c)^{\alpha(abi)}_{\beta(j)} \rightarrow (Q_c)^{\alpha(ab)}_{\beta(ij)} \tag{9.27}$$

We will need a general mapping function that can be used regardless of the amount of states used. It turns out that we can use the same mapping as before, just generalized to N states.

$$\alpha(p_1, p_2, p_3, ..., p_N) = p_1 + p_2 N_1 + p_3 N_1 N_2 + ... + p_N N_1 N_2 ... N_{N-1} \tag{9.28}$$

Where N_n determines the maximum number of states for p_n. If for example $p_n \in i$, i.e. p_n is a hole-state, $N_n = N_{holes}$.

Writing the diagrams as matrix-matrix multiplications serves as a significant reduction of computational time, due to the efficient algortithms in the BLAS-packages for matrix-matrix multiplications. However, since one has to save all the matrices, memory usage will be a problem for large basises.

9.3 Block Implementation

One can both greatly reducing memory usage and improve computational speed by exploiting symmetries for infinite matter . Due to kroenecker delta's in the interaction, one such symmetry is the conservation of momentum

$$\delta_{\mathbf{k}_p+\mathbf{k}_q,\mathbf{k}_r+\mathbf{k}_s} \rightarrow \mathbf{k}_p + \mathbf{k}_q = \mathbf{k}_r + \mathbf{k}_s \tag{9.29}$$

We also conserve spin

$$m_{s_p} + m_{s_q} = m_{s_r} + m_{s_s} \tag{9.30}$$

and for nuclear matter, we will conserve isospin aswell

$$m_{t_p} + m_{t_q} = m_{t_r} + m_{t_s} \tag{9.31}$$

The amplitudes will be subject to the same restrictions, vizualised by the first order amplitude generated by perturbation theory

$$(t^{ab}_{ij})^{t=0} = \frac{\langle ab|\hat{v}|ij\rangle}{\epsilon_i + \epsilon_j - \epsilon_a - \epsilon_b} \tag{9.32}$$

Looking at the L_a term

$$L_a = \sum_{cd} \langle ab|\hat{v}|cd\rangle \, t^{ab}_{ij} \tag{9.33}$$

We see that

$$\mathbf{k}_a + \mathbf{k}_b = \mathbf{k}_c + \mathbf{k}_d = \mathbf{k}_i + \mathbf{k}_j \tag{9.34}$$

And the same for spin

$$m_{s_a} + m_{s_b} = m_{s_c} + m_{s_d} = m_{s_i} + m_{s_j} \tag{9.35}$$

When summing over all variations of contractions, only the quantum numbers preserving the symmetry requirements are nonzero. When storing the interactions in a matrix, most of it will have zero-elements. The blocking method will store the nonzero parts in blocks inside the matrix. By keeping track of the blocks, we can reduce the full matrix-matrix multiplication to a series of multiplications of the blocks. We will hereby refer to the series of blocks as *channels*.

9.3.1 Two-state configurations

As we can see from the L_a diagram, the conservation laws apply for a combination of two states. The next step is then to set up all two-state configurations that will be needed. We start by setting up the direct two-state channels, T, which consist of all two-hole and two-particle configurations. A unique identifier must be set up for the combination of quantum numbers. The identifier is used to aligning the non-zero combinations of two-body states to the same channel. Without this identifier, we will have to loop over all channels for each two-body state. I have used the following function

$$\begin{aligned} \text{Index}(N_x, N_y, N_z, S_z, T_z) =& 2(N_x + m)M^3 + 2(N_y + m)M^2 + & (9.36)\\ & 2(N_z + m)M + 2(S_z + 1) + (T_z + 1) & (9.37) \end{aligned}$$

Using the same logic as in equation (9.3) to get a unique identifier for every combination of N_x, N_y, N_z, S_z and T_z. Which imply that the two-body states have the same momentum, spin and isospin projection, which satisfies our conservation laws. We need m and M to be sufficiently large. I have used

$$m = 2|\sqrt{N_{\max}}| \quad M = 2m + 1 \tag{9.38}$$

Because of the Pauli-exclusion, two particles cannot occupy the same state, so we can further reduce the amount of two-body states by excluding equal one-body states from the channels. An algorithm for setting up the direct channels can be

portraied as

for one-body state 1 $\in$ STATES :
  for one-body state 2 $\in$ STATES :
    if one-body state 1 $\neq$ one-body state 2 :
    $N_x = n_{x,1} + n_{x,2}$
    $N_y = n_{y,1} + n_{y,2}$
    $N_z = n_{z,1} + n_{z,2}$
    $S_z = m_{s,1} + m_{s,2}$
    $T_z = m_{t,1} + m_{t,2}$
    $\mathrm{Id} = \mathrm{Index}(N_x, N_y, N_z, S_z, T_z)$
    $T \leftarrow (\text{ one-body state 1, one-body state 2, Id})$

9.3.2 Unaligned channels

Diagram L_a, L_b and Q_a have conservation requirements as shown previously for L_a

$$\mathbf{k}_a + \mathbf{k}_b = \mathbf{k}_c + \mathbf{k}_d = \mathbf{k}_i + \mathbf{k}_j \tag{9.39}$$

Which are implemented using the direct channels. We will however run into some trouble when computing the unaligned diagrams L_c, Q_b, Q_c and Q_d. The L_c diagram is given by

$$L_c = -\hat{P}(ij|ab) \sum_{kc} \langle kb|\hat{v}|cj\rangle \, t_{ik}^{ac} \tag{9.40}$$

Looking at the conservation requirement for L_c

$$\mathbf{k}_k + \mathbf{k}_b = \mathbf{k}_c + \mathbf{k}_j = \mathbf{k}_a + \mathbf{k}_c = \mathbf{k}_i + \mathbf{k}_k \tag{9.41}$$

and

$$m_{s,k} + m_{s,b} = m_{s,c} + m_{s,j} \qquad m_{t,k} + m_{t,b} = m_{t,c} + m_{t,j} \tag{9.42}$$

When realigning the equation, we want it to be

$$\tilde{L}c = -\hat{P}(ij|ab) \sum_{kc} \langle bj|\tilde{v}|ck\rangle \, \langle ck| \, \tilde{t} \, |ai\rangle \tag{9.43}$$

We reorganize the conservation requirements as well to make sure we only calculate the non-zero terms

$$\mathbf{k}_b - \mathbf{k}_j = \mathbf{k}_c - \mathbf{k}_k = \mathbf{k}_c - \mathbf{k}_k = \mathbf{k}_i - \mathbf{k}_a \tag{9.44}$$

Spin and isospin will be subject to the same reorganizing. We see that the direct channels do not represent the right conservation requirement and we must set up the cross channels, X, that consist of particle-hole or hole-particle two-body configurations. An algorithm can be set up as

for one-body state 1 $\in$ STATES :
 for one-body state 2 $\in$ STATES :
  if one-body state 1 $\neq$ one-body state 2 :
  $N_x = n_{x,1} - n_{x,2}$
  $N_y = n_{y,1} - n_{y,2}$
  $N_z = n_{z,1} - n_{z,2}$
  $S_z = m_{s,1} - m_{s,2}$
  $T_z = m_{t,1} - m_{t,2}$
  Id = Index$(N_x, N_y, N_z, S_z, T_z)$
  $X \leftarrow$ (one-body state 1, one-body state 2, Id)
  Id$'$ = Index$(-N_x, -N_y, -N_z, -S_z, -T_z)$
  $X' \leftarrow$ (one-body state 2, one-body state 1, Id')

Where X' is the cross channel compliment, $X(pq) = X'(qp)$. The coss-channels are used for calculating Q_b and L_c.

Looking at the diagram Q_c

$$Q_c = -\frac{1}{2}\hat{P}(ij)\sum_{klcd}\langle kl|\hat{v}|cd\rangle\, t_{ik}^{ab}t_{jl}^{cd} \tag{9.45}$$

With the momentum conservation requirement

$$\mathbf{k}_k + \mathbf{k}_l = \mathbf{k}_c\mathbf{k}_d = \mathbf{k}_i + \mathbf{k}_k = \mathbf{k}_a + \mathbf{k}_b = \mathbf{k}_j + \mathbf{k}_l = \mathbf{k}_c + \mathbf{k}_d \tag{9.46}$$

We see that we must realign the diagram as

$$\tilde{Q}_c = -\frac{1}{2}\hat{P}(ij)\sum_{klcd}\langle abi|\,\tilde{t}\,|k\rangle\,\langle k|\,\tilde{v}\,|cdl\rangle\,\langle cdl|\,\tilde{t}\,|j\rangle \tag{9.47}$$

Which set the conservation requirement as

$$\mathbf{k}_a + \mathbf{k}_b - \mathbf{k}_i = \mathbf{k}_k = \mathbf{k}_k = \mathbf{k}_c + \mathbf{k}_d - \mathbf{k}_l = \mathbf{k}_c + \mathbf{k}_d - \mathbf{k}_l = \mathbf{k}_j \tag{9.48}$$

We set up three-body and corresponding one-body channels to calculate Q_c and Q_d. An example algorithm for the K_h and $K_{p,p,h}$ channels can be outlined as

for one-body state 1 $\in$ HOLES :
$N_x = n_{x,1}$
$N_y = n_{y,1}$
$N_z = n_{z,1}$
$S_z = m_{s,1}$
$T_z = m_{t,1}$
Id = Index$(N_x, N_y, N_z, S_z, T_z)$
$K_h \leftarrow$ (one-body state 1, Id)

for one-body state 1 $\in$ PARTICLES :
for one-body state 2 $\in$ PARTICLES :
for one-body state 3 $\in$ HOLES :
if one-body state 1 $\neq$ one-body state 2 :
$N_x = n_{x,1} + n_{x,2} - n_{x,3}$
$N_y = n_{y,1} + n_{y,2} - n_{y,3}$
$N_z = n_{z,1} + n_{z,2} - n_{z,3}$
$S_z = m_{s,1} + m_{s,2} - n_{s,3}$
$T_z = m_{t,1} + m_{t,2} - n_{t,3}$
Id = Index$(N_x, N_y, N_z, S_z, T_z)$
$K_{p,p,h} \leftarrow$ (one-body state 1, one-body state 2, one-body state 3, Id)

9.3.3 Permutations

Some diagrams come with permutations. These are easy to handle by simply interchanging indexes when adding the diagram to $t^{(n+1)}$.

for i $\in$ Holes :
 for j $\in$ Holes :
  for a $\in$ Particles :
   for b $\in$ Particles :
    $t^{(n+1)}(a,b,i,j) = t^{(n+1)} - \frac{1}{2}\left(Q_c(a,b,i,j) - Q_c(a,b,j,i)\right)$

9.4 Setting Up Basis

Before doing coupled cluster calculations, the basis must be set up. An important property of this basis, is the occupied and virtual states. For infinite nuclear matter, the following algorithm can be used to set up the states. This algorithm should reproduce the magic numbers presented.

for shell $\in$ All Shells :
 for $n_x, n_y, n_z \in$ [$-$shell, shell] :
  $n = n_x^2 + n_y^2 + n_z^2$
  if $n =$ shell :
   for $m_s \in \{-1, 1\}$
    for $m_t \in \{-1, 1\}$
     States $\leftarrow (e, n_x, n_y, n_z, m_s, m_t)$
     $N_s = N_s + 1$
     if shell $<$ Fermi level :
      $N_h = N_h + 1$

9.5 Parallellization

To fully utilize the computational power in modern processors, one must use a parallellized code. Modern processors usually come with more than one core to save power output at the same effiency [22]. A standard written C++ program will be processed using only 1 *thread*, meaning that a single core only will be used.

The super computer, *Smaug*, located at the Institute of Physics at the University of Oslo is built of processors with many but low performing cores given todays standards. If one can split the program into multiple threads, each executed at the same time in different cores, one can hope to reduce computational time substansially.

Chapter 10

Results

10.1 The Pairing Model

The Pairing Model serve as a valuable benchmark for implemented solvers. As I have looked at a 4p4h configuration, a full configuration interaction solver can be implemented giving the exact solution. One can also calculate the exact solution for second order perturbation theory by hand [7].

$$\Delta E_{MBPT2} = \frac{1}{4}\sum_{abij}\frac{\langle ij||ab\rangle\langle ab||ij\rangle}{\epsilon_{ij}^{ab}} = \sum_{a<b,i<j}\frac{\langle ij||ab\rangle\langle ab||ij\rangle}{\epsilon_{ij}^{ab}} \tag{10.1}$$

Where

$$\epsilon_{ij}^{ab} = \epsilon_i + \epsilon_j - \epsilon_a - \epsilon_b \tag{10.2}$$

and

$$\epsilon_p = h_{pp} + \sum_i \langle pi||pi\rangle \tag{10.3}$$

This results in

$$\Delta E_{MBPT2} = \frac{\langle 01||45\rangle^2}{\epsilon_{01}^{45}} + \frac{\langle 01||67\rangle^2}{\epsilon_{01}^{67}} + \frac{\langle 23||45\rangle^2}{\epsilon_{23}^{45}}\ \frac{\langle 23||67\rangle^2}{\epsilon_{23}^{67}} \tag{10.4}$$

$$\Delta E_{MBPT2} = -\frac{g^2}{4}\left(\frac{1}{4+g} + \frac{1}{6+g} + \frac{1}{2+g} + \frac{1}{4+g}\right) \tag{10.5}$$

Where g represents the interaction strength. The table below shows my results for various g's both using the exact mbpt2 calculations and my numerically computed results. All results can be accessed on github [23]

g	E_0	exact ΔE_{MBPT2}	ΔE_{MBPT2}
-1	3	-0.466667	-0.466667
-0.5	2.5	-0.0887446	-0.0887446
0	2	0	0
0.5	1.5	-0.0623932	-0.0623932
1	1	-0.219048	-0.219048

Table 10.1: A table showing corrolation energies for Pairing model with 4 particle-states and 4 hole-states.

g	ΔE_{MBPT2}	$\Delta E^{(1)}_{CCD}$
-1	-0.466667	-0.466667
-0.5	-0.0887446	-0.0887446
0	0	0
0.5	-0.0623932	-0.0623932
1	-0.219048	-0.219048

Table 10.2: A table comparing corrolation energies for Pairing model with 4 particle-states and 4 hole-states. This table show that CCD solver used with only a single iteration produces results exactly equal to mbpt2. This was done with the naive implementation of CCD equations

As one can see, the corrolation energies computed perfectly matches which both tells us that the basis set is set up correctly and that the MBPT2 solver is set up correctly. The results presented also match the results found in [7]

The second order perturbation theory is valuble for benchmarking my implementation of Coupled Cluster Doubles. By initializing the first set of amplitudes, t, as zero, I get

$$t_{ij}^{ab(0)} = 0 \tag{10.6}$$

$$t_{ij}^{ab(1)} = \frac{1}{4}\sum_{ijab}\frac{\langle ab||ij\rangle}{\epsilon_{ij}^{ab}} \tag{10.7}$$

Which is equal to second order pertubation theory.

10.1.1 Comparison of CCD solvers

In this thesis I have created three different solvers for Coupled Cluster Doubles equations.

g	ΔE_{CCD} Naive	ΔE_{CCD} Intermediates
0	x	x
-0.5	-0.0630564	-0.0630562
0	0	0
0.5	-0.0833621	-0.0833623
1	-0.369557	-0.369557

Table 10.3: A table comparing corrolation energies for Pairing model with 4 particle-states and 4 hole-states. This table compare results from Naive and Intermediate implementation of CCD equations. A relaxing factor of $w = 0.3$ has been used because of divergence around $g = -1$

1. A naive brute force implementation of the equations summing over all variables.

2. A naive brute force implementation of intermediate equations summing over all variables.

3. Rewriting summations as matrix-matrix multiplications and exploiting various symmetry arguments one can set up a block implementation.

As shown in table (10.2), the naive implementation reproduces the mbpt2 energies as expected. I have used both the naive and intermediate CCD solver to compute corrolation energies for the Pairing model and again, [7] provides us with a good benchmark for the CCD equations.

As one can see, my solvers reproduce results presented in [7]. For values of g close to -1, one will see a divergence for CCD equations. By introducing a relaxing factor of $w = 0.3$, this problem was solved.

10.1.2 Comparison of various solvers

The full configuration interaction provides us with the exact solution for the 4p4h Pairing model. It can therefore be useful to compare the performance of Perturbation theory to second, third and fourth order with Coupled Cluster Doubles and configuration interaction without the four-particle excitation.

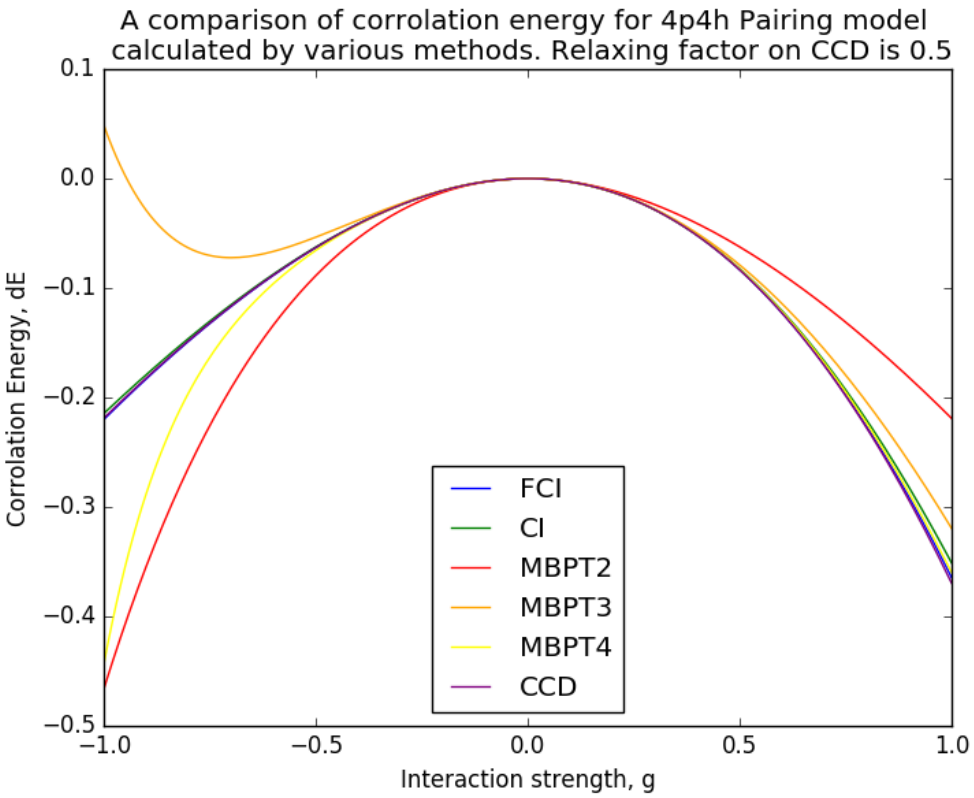

H

Figure 10.1: Comparing

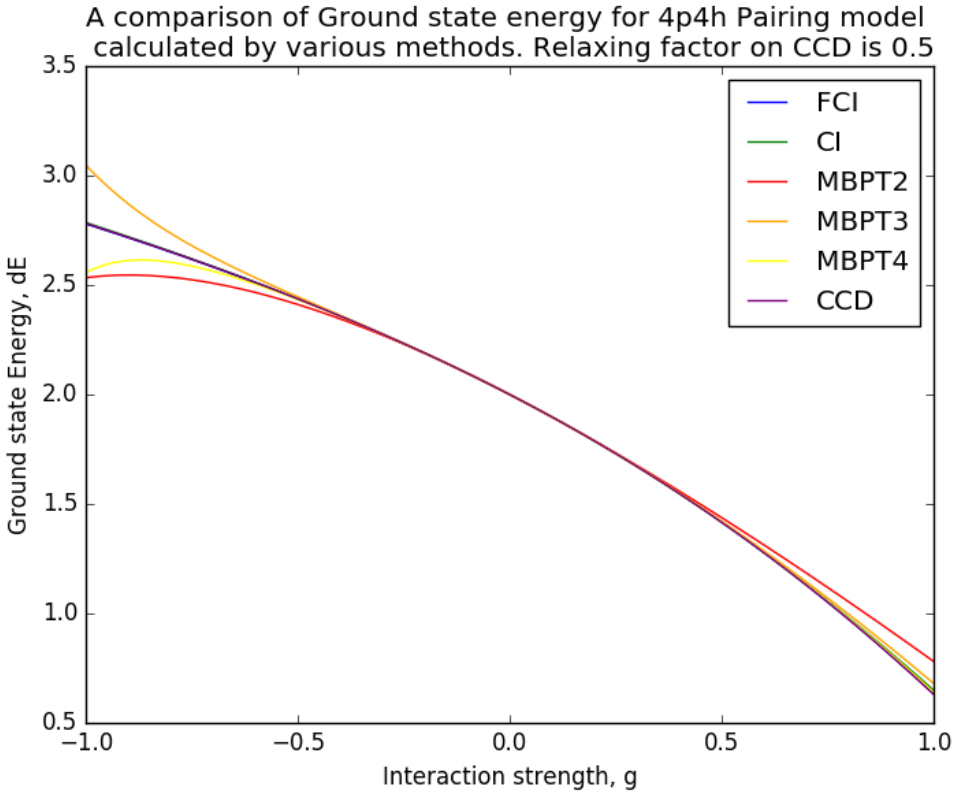
A comparison of Ground state energy for 4p4h Pairing model
calculated by various methods. Relaxing factor on CCD is 0.5
Ground state Energy, dE
Interaction strength, g
FCI
CI
MBPT2
MBPT3
MBPT4
CCD
3.5
3.0
2.5
2.0
1.5
1.0
0.5
−1.0
−0.5
0.0
0.5
1.0

Figure 10.2

Chapter 11

Conclusion and future prospects

Bibliography

[1] Gustav Baardsen *Coupled-cluster theory for infinite matter* 2014

[2] Audun Skau Hansen *Coupled Cluster studies of infinite systems,* Master thesis, University of Oslo, 2015

[3] Isaiah Shavitt and Rodney J. Bartlett *Many-Body Methods in Chemistry and Physics* 2009

[4] Attila Szabo and Neil S. Ostlund *Modern Quantum Chemistry. Introduction to Advanced Electronic Structure Theory* 1982

[5] David J. Griffiths *Introduction to Quantum Mechanics* Second edition 2005

[6] J.J. Sakurai *Modern Quantum Mechanics* Revised Edition 1993

[7] Morten Hjorth-Jensen, Maria Paola Lombardo and Ubiraja van Kolck *An Advanced Course in Computational Nuclear Physics* 2016

[8] Stanley Raimes *Many-Electron Theory* 1972

[9] Leonard Susskind and Art Friedman *Quantum Mechanics, The Theoretical Minimum* 2014

[10] T. Daniel Crawford and Henry F. Schaefer III *An Introduction to Coupled Cluster Theory for Computational Chemists*

[11] B. D. Day *Rev. Mod. Phys.,* 39:719, 1967.

[12] D. R. Thompson, M. Lemere and Y.C. Tang. *Nucl. Phys. A,* 286:53 1977.

[13] J. J. Shepherd, A. Grneis, G.H. Booth, G. Kresse and A. Alavi *Phys. Rev. B,* 86:035111, 2012.

[14] J.J. Shepherd and A. Grneis *Phys. Rev. Lett.,* 110:226401, 2013.

[15] N. D. Drummond, R. J. Needs, A. Sorouri and W. M. C. Foulkes *Phys. Rev. B,* 78:125106

[16] L. M. Fraser, W. M. C. Foulkes, G. Rajagopal, R. J. Needs, S.D. Kenny and A. J. Williamson *Phys. Rev. B,* 53:1814, 1996

[17] P.P. Ewald. Die berechnung optischer und elektrostatischer gitterpotentiale. *Annalen der Physik,* 369(3), 1921. ISSN 1521-3889. doi: 10.1002/andp.19213690304

[18] Hans Petter Langtangen *A Primer on Scientific Programming with Python* Scond Edition, Springer 2011

[19] William H. Press, Saul A. Teukolsky, William T. Vetterling, Brian P. Flannery *Numerical Recipes, The Art of Scientific Computing* Third Edition, Cambridge 2007

[20] Morten Hjorth-Jensen *Nuclear Shell Model, Nuclear Talent course 2* URL (14. july, 2016): http://nucleartalent.github.io/Course2ManyBodyMethods/doc/pub/fci/pdf/fci-print.pdf

[21] Carlo Barbieri, Wim Dickhoff, Gaute Hagen, Morten Hjorth-Jensen, Artur Polls *Many-body Methods for Nuclear Physics, Nuclear Talent course 2* URL: *http://nucleartalent.github.io/Course2ManyBodyMethods/doc/web/course.html*

[22] Tim Mattson *Intel Youtube Course in OpenMp: Introduction to OpenMP - Tim Mattson (Intel)* URL: *https://www.youtube.com/playlist?list=PLLX-Q6B8xqZ8n8bwjGdzBJ25X2utwnoEG.*

[23] Fredrik Wilhelm Holmen *https://github.com/wholmen/Master*

[24] Conrad Sanderson. Armadillo: An open source c++ linear algebra library for fast prototyping and computationally intensive experiments, 2010. URL: *http://arma.sourceforge.net/docs.html.*